All the transduction assays in this study were performed at a multiplicity of infection (MOI) of 1.

In some experiments, purified mAbs against CD49d and/or CD49e (1 μg/ml, Beckman Coulter; both capable of inhibiting the cell adhesion mediated by their target molecule) were added to the culture 10 min before MLV-derived retroviral induction to assess the effect of inhibition of integrin-mediated cell adhesion.

The colony assay was performed with Methocult GF+ H4435 (StemCell Technologies, Northampton, UK). After MLV-derived retroviral transduction, 3×10^2 $CD34^+$ cells were suspended on 1 ml of Methocult and plated in 35-mm dishes. The number of colonies comprising more than 50 cells, including erythroid colonies, was scored after incubation for 21 days. The experiments were performed in triplicate, and colony numbers (means $\pm$ SD) are indicated in Table 1.

Immunofluorescence study

After cultivation periods the cells were stained with fluorescence-labeled mAbs and analyzed by flow cytometry as described previously (Kiyokawa *et al.*, 1990). A three-color immunofluorescence study was performed with a combination of PE, PC-5, and GFP introduced by MLV-derived retroviral vectors. Experiments were performed in triplicate, and means and standard deviations of the cell counts are indicated in the figures.

Results

Expression of integrins on $CD34^+$ cells on the course of MLV-derived retroviral transduction

As shown in Fig. 1, we first confirmed that the recombinant fibronectin fragment CH-296 is effective for transduction of $CD34^+$ cells with an MLV-derived retroviral vector for GFP

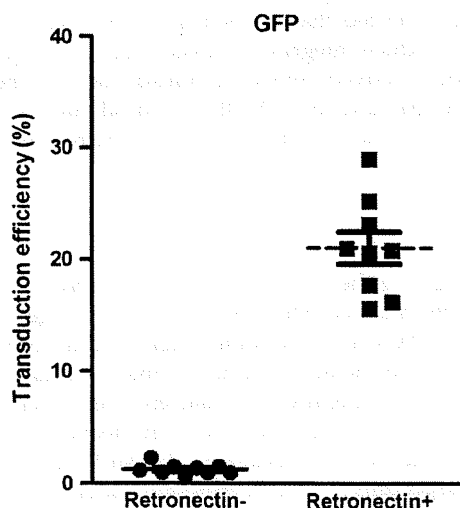

FIG. 1. Effect of CH-296 (RetroNectin) on murine leukemia virus (MLV)-derived retrovirus-mediated green fluorescent protein (GFP) gene introduction. $CD34^+$ cells were transduced with an MLV-derived retroviral vector for GFP expression in the absence (*left*) or presence (*right*) of the recombinant fibronectin fragment CH-296, as described in Materials and Methods, by means of a single exposure. Subsequent GFP expression was tested by flow cytometry. Results are expressed as means $\pm$ SD.

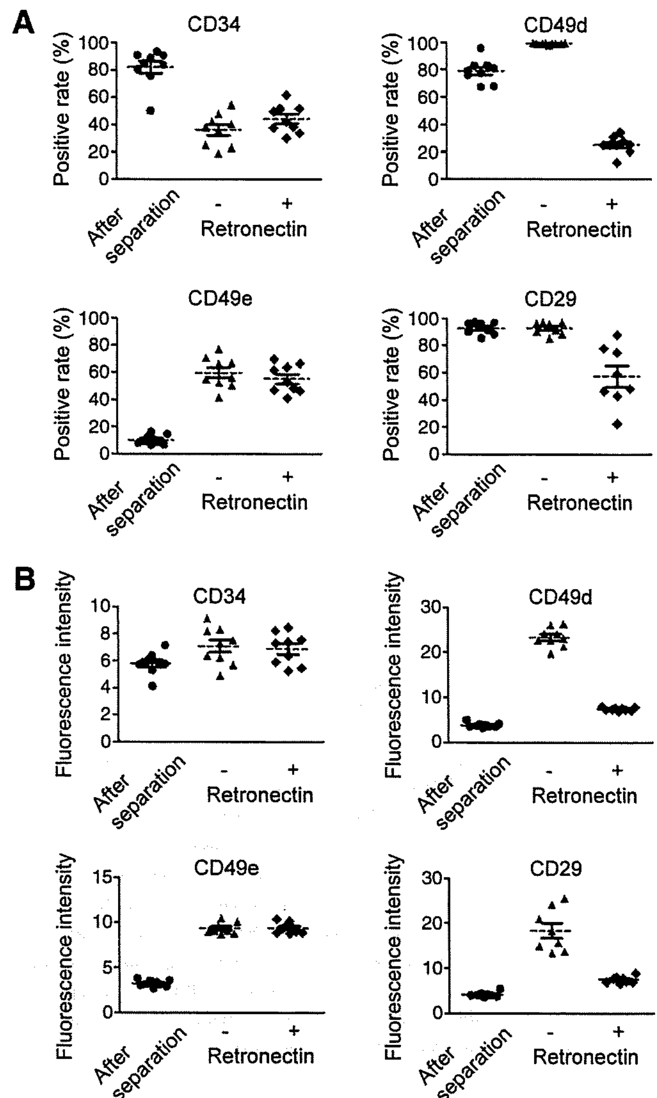

FIG. 2. Expression of VLA-4 and VLA-5 in the course of MLV-derived retroviral transduction of $CD34^+$ cells. Expression of VLA-4 and VLA-5 on $CD34^+$ cells before (*left*) and after *ex vivo* culture for MLV-derived retroviral transduction in the absence (*middle*) or presence (*right*) of CH-296 was examined by flow cytometry, using specific antibodies as indicated. (**A**) Positive rates and (**B**) mean fluorescence intensities are shown as means $\pm$ SD.

expression. After transduction with a single exposure to fresh viral supernatant, almost no GFP expression was observed in $CD34^+$ cells in the absence of CH-296, whereas when the dish precoated with CH-296 was used, about 20% of the cells (15.6 to 29.0%; mean, 21.0 $\pm$ 3.1%) expressed GFP in repeated experiments (Fig. 1), indicating that CH-296 was indeed effective for MLV-derived retroviral transduction of $CD34^+$ cells.

We therefore tested $CD34^+$ cells for integrin expression during MLV-derived retroviral transduction. As shown in Fig. 2A, when freshly isolated $CD34^+$ cells were tested for expression of CD49d, a component of VLA-4, the percentage of positive cells was already about 80% (67.6 to 96.0%; mean, 79.1 $\pm$ 6.0%), but it rose to approximately 100% during culture

with the combination of cytokines for MLV-derived retroviral transduction. Moreover, comparison of the mean fluorescence intensity of CD49d in the positive cells showed a significant increase after the culture periods (Fig. 2B). Testing CD34$^+$ cells for expression of CD49e, a component of VLA-5, revealed a low positive rate and mean fluorescence intensity when first isolated, but they both increased significantly after cultivation for transduction. A significant level of expression of CD29, another component of both VLA-4 and VLA-5, was found in freshly isolated CD34$^+$ cells, but the mean fluorescence intensity still increased in the course of cultivation for MLV-derived retroviral transduction. The data indicate that the levels of VLA-4 and VLA-5 in freshly isolated CD34$^+$ cells were not always high, but that the intensity of expression of both molecules significantly increased in the course of MLV-derived retroviral transduction.

Interestingly, although integrin expression was significantly increased by cultivation with the cytokine cocktail, it was significantly reduced in the presence of CH-296 (Fig. 2). The degree of reduction was more significant for CD49d expression, but the decrease in CD49e expression was less marked (Fig. 2).

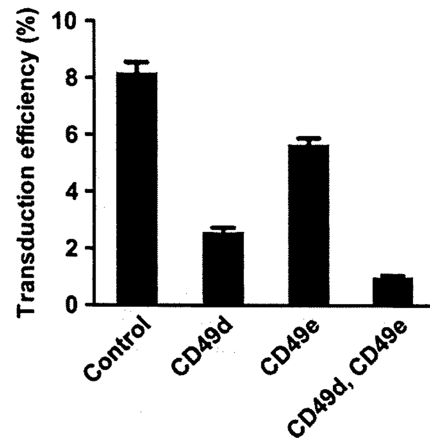

FIG. 3. Effect of inhibition of integrin-mediated attachment to CH-296 on the efficiency of transduction of CD34$^+$ cells with MLV-derived retroviral vector. CD34$^+$ cells were transduced with MLV-derived retroviral vector for GFP expression in the presence of CH-296 as described in Fig. 1. Antibody against CD49d, CD49e, or both was added to the cells before exposure to the virus, and their effects were examined as described in Materials and Methods.

Role of integrins in CH-296-based MLV-derived retroviral transduction of CD34$^+$ cells

We next investigated whether the integrins are indeed involved in the CH-296-based MLV-derived retroviral transduction of CD34$^+$ cells. When anti-CD49d antibody, which inhibits cell adhesion via CD49d, was added to the culture, transduction efficiency was significantly reduced (Fig. 3). The anti-CD49e antibody similarly reduced the transduction efficiency (Fig. 3), and when both antibodies were added at the same time, a synergistic effect in reducing transduction efficiency was observed. The data indicate that the integrins expressed on CD34$^+$ cells are indeed important to CH-296-based MLV-derived retroviral transduction.

Effect of cytokines on integrin levels on CD34$^+$ cells

We next attempted to identify the cytokines in the cocktail that were responsible for inducing expression of the integrins during the course of MLV-derived retroviral transduction. Both the positive rates and the fluorescence intensity measurements showed that SCF, TPO, and FL each increased expression of CD49d, but their effects were limited (Fig. 4A and B). SCF was the most effective of the three cytokines in enhancing CD49d expression. Exposure to a combination of IL-6 and sIL-6R had a weaker effect on CD49d expression than SCF, TPO, and FL alone (Fig. 4A and B). When SCF and TPO were combined, however, the level of CD49d expression increased significantly, and as shown in Fig. 4A and B, the positive rate and fluorescence intensity of CD49d on CD34$^+$ cells cultured with the combination of SCF and TPO were almost the same as when cultured with the complete cocktail of five factors. In addition, the cytokines enhanced CD49e expression to the same extent as the cytokine-induced expression of CD49d (Fig. 4C and D).

We then examined the effect of the cytokines on transduction efficiency with the GFP-expressing MLV-derived retroviral vector. Flow cytometry showed that the degree of GFP expression after transduction with SCF and TPO was comparable to that achieved with the full cocktail, whereas no significant GFP expression was observed after transduction with SCF, TPO, or FL alone or with the IL-6 and sIL-6R combination (Fig. 4E). When transduction efficiency was tested by colony assay, the effect of SCF and TPO was more prominent (Table 1), and the colony assay also showed that the SCF and TPO combination could maintain progenitor cells with colony-forming ability at a level comparable to that achieved with the complete cocktail.

The data indicated that the SCF and TPO combination is sufficient to induce integrin expression that is adequate for effective MLV-derived retroviral transduction in the presence of CH-296, and that FL, IL-6, and sIL-6R are not essential for transduction of MLV-derived retroviruses with CH-296.

Discussion

Introduction of the recombinant human fibronectin fragment CH-296 into the MLV-derived retroviral gene transduction of HSPCs has contributed significantly to progress in stem cell gene therapy and has enabled success in clinical trials of gene therapy for children with inherited immunodeficiencies (Ariga *et al.*, 2001). In theory the effect of CH-296 is achieved by colocalizing the MLV-derived retrovirus and target cells of specific adhesion domains of CH-296, including integrin-binding sites (Hanenberg *et al.*, 1996). Although the efficacy of this method for MLV-derived retroviral gene transduction of human HSPCs has been confirmed in a number of experiments *in vitro* (Murray *et al.*, 1999), the actual role of the integrins expressed on HSPCs had not been analyzed. In the present study we investigated the kinetics of VLA-4 and VLA-5 expression on CD34$^+$ cells during *ex vivo* culture for MLV-derived retroviral gene transduction

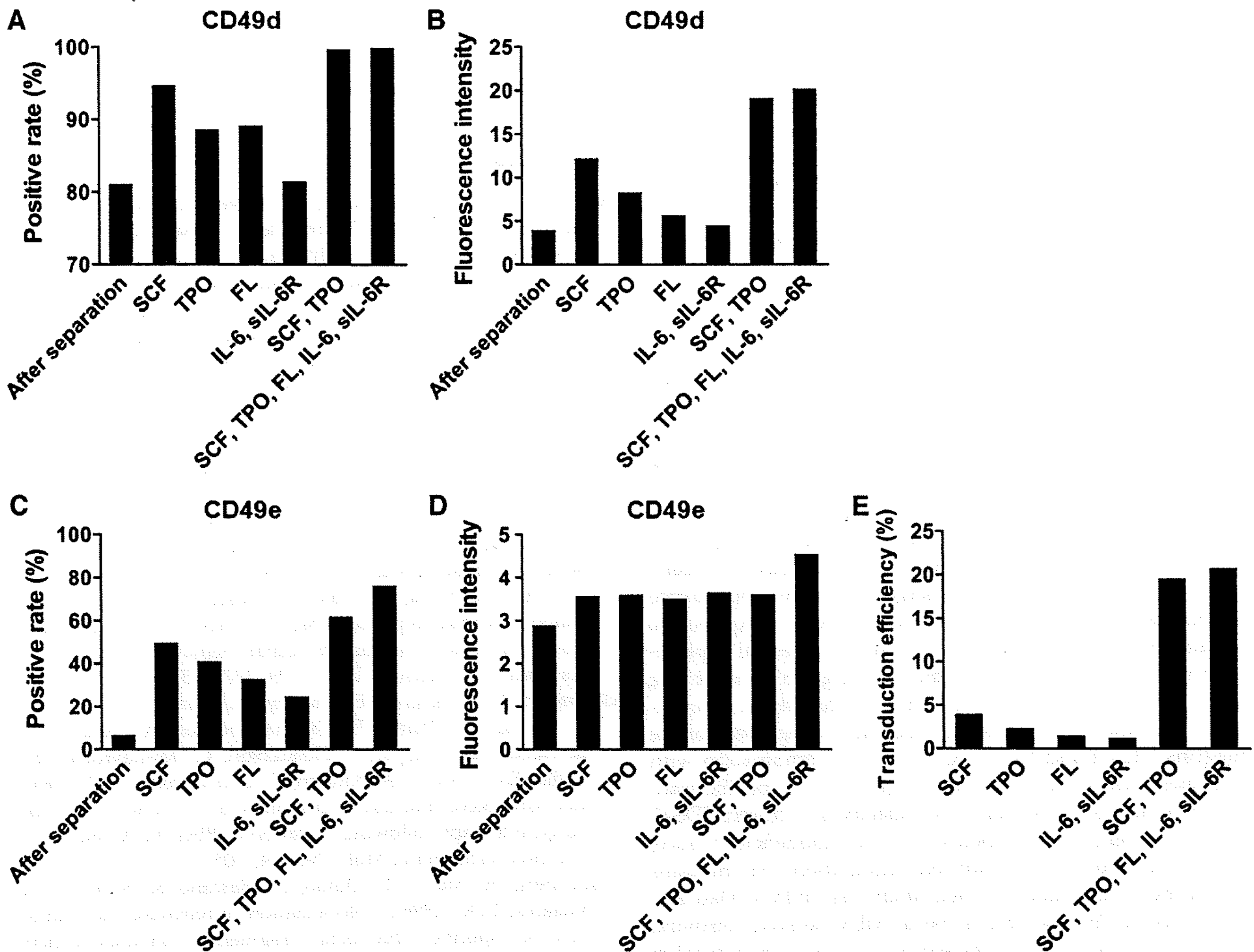

FIG. 4. Effect of cytokines on CD49d and CD49e expression on $CD34^+$ cells. $CD34^+$ cells were cultured in the presence of the cytokines indicated, and the expression of CD49d and CD49e was examined as described in Fig. 2. (**A** and **C**) Positive rates and (**B** and **D**) mean fluorescence intensities of CD49d and CD49e are shown. The experiments were performed in duplicate. (**E**) CH-296-based transduction efficiency with the MLV-derived retroviral vector for GFP expression in each culture was examined as in Fig. 1.

and demonstrated the importance of integrins for efficient transduction.

As demonstrated in this study, use of either the anti-CD49d antibody or anti-CD49e antibody, both of which are capable of inhibiting integrin-mediated cell adhesion, led to a reduction in the efficiency of transduction with the MLV-derived retroviral vector (Fig. 3). Because culture conditions insufficient to enhance CD49d expression on $CD34^+$ cells were found to result in extremely low gene transduction (Fig. 4E), abundant levels of integrins VLA-4 and VLA-5 are required for the effective transduction of MLV-derived retroviral vectors. Interestingly, CD49d expression on the surface of $CD34^+$ cells has been shown to be significantly downregulated during treatment with MLV-derived retroviral gene transduction in the presence of CH-296, and the magnitude of the downregulation was far greater than that of CD49e expression. Because downregulation of integrins is thought to indicate adhesion-mediated activation of integrin signaling (Pellinen and Ivaska, 2006), our data indicate that VLA-4 is more effectively activated in the presence of CH-296. We also observed that the anti-CD49d antibody inhibited MLV-derived retroviral gene transduction more effectively than the anti-CD49e antibody did. Thus, our findings indicate that VLA-4 plays a more important role in CH-296-mediated MLV-derived retroviral gene transduction than VLA-5 does, although more detailed experiments are needed to be able to draw a definite conclusion.

The levels of VLA-4 and VLA-5 on $CD34^+$ cells are quite low immediately after purifying the cells from a source such as cord blood, and they are insufficient for effective MLV-derived retroviral gene transduction. As we demonstrated in this study, the cells must be cultured with certain cytokines to yield adequate integrin levels for effective MLV-derived retroviral transduction. Therefore, pretransduction culture

is needed not only to introduce cells into the cell cycle but also to induce sufficient expression of VLA-4 and VLA-5 on CD34$^+$ cells. It is also important to be able to induce the expression of VLA-4 and VLA-5 with only a limited number of cytokines, and we determined that a combination of SCF and TPO is the minimum required for sufficient expression of integrins to achieve effective MLV-derived retroviral gene transduction.

A combination of SCF, TPO, FL, and IL-3 is commonly used for MLV-derived retroviral gene transduction, and a combination of SCF, TPO, FL, IL-6, and soluble IL-6 receptor has proven useful for stem cell gene therapy to treat ADA deficiency. Although both cocktails are able to maintain stem cells or progenitor cells and supply a sufficient number of target cells in which the defective gene has been replaced (Ariga *et al.*, 2001; Gaspar *et al.*, 2006), they induce significant expression of CD33, a myeloid marker antigen, in most CD34$^+$ cells during the course of MLV-derived retroviral gene transduction (data not shown). Because our data indicate that the combination of SCF and TPO is sufficient to induce adequate integrin expression to achieve effective MLV-derived retroviral gene transduction, it is worth investigating more appropriate combinations of cytokines based on these two, to expand the population of progenitor cells for more successful replacement with functionally complemented target cells according to the lineage of the defective cells in each disease. Interestingly, Dao and Nolta have reported that engagement of the integrins VLA-4 and VLA-5 to CH-296 in combination with cytokines induces up- and downregulation of specific transcription factors and sustains the capacity of cultured CD34$^+$ cells to undergo hematopoiesis in immunodeficient mice, suggesting that CH-296-induced stimulation via integrins affects the maintenance of their ability as HSPCs (Dao and Nolta, 2007). The use of CH-296 in MLV-derived retroviral gene transduction should therefore not only be beneficial in terms of achieving higher transduction efficiency but in maintaining HSPCs.

In conclusion, we confirmed that expression of VLA-4 and VLA-5 on HSPCs is necessary for effective CH-296-based MLV-derived retroviral gene transduction and that a combination of cytokines is important to inducing expression of integrins on HSPCs. Our results should aid in the development of a more successful protocol of MLV-derived retroviral gene transduction for stem cell gene therapy with CH-296.

Acknowledgments

The authors thank the Tokyo Cord Blood Bank for the distribution of cord blood for research use. This work was supported by Health and Labor Sciences Research grants (Research on Children and Families [H19-003 and H18-005], the third term comprehensive 10-year-strategy for cancer control [H19-010], Research on Human Genome Tailor Made and Research on Publicly Essential Drugs and Medical Devices [H18-005]) from the Ministry of Health, Labor, and Welfare of Japan. It was also supported by a grant from the Japan Health Sciences Foundation for Research on Publicly Essential Drugs and Medical Devices (KHA1004), and by a Child Health and Development grant from the Ministry of Health, Labor, and Welfare of Japan. The study was also supported by CREST, JST.

Author Disclosure Statement

No competing personal or financial interests exist for any of the authors in relation to this manuscript.

References

Ariga, T., Oda, N., Yamaguchi, K., Kawamura, N., Kikuta, H., Taniuchi, S., Kobayashi, Y., Terada, K., Ikeda, H., Hershfield, M.S., Kobayashi, K., and Sakiyama, Y. (2001). T-cell lines from 2 patients with adenosine deaminase (ADA) deficiency showed the restoration of ADA activity resulted from the reversion of an inherited mutation. Blood 97, 2896–2899.

Bodine, D.M., Dunbar, C.E., Girard, L.J., Seidel, N.E., Cline, A.P., Donahue, R.E., and Orlic, D. (1998). Improved amphotropic retrovirus-mediated gene transfer into hematopoietic stem cells. Ann. N. Y. Acad. Sci. 30,139–150.

Cavazzana-Calvo, M., Hacein-Bey, S., de Saint Basile, G., Gross, F., Yvon, E., Nusbaum, P., Selz, F., Hue, C., Certain, S., Casanova, J.L., Bousso, P., Deist, F.L., and Fischer A. (2000). Gene therapy of human severe combined immunodeficiency (SCID)-X1 disease. Science 288, 669–672.

Dao, M.A., and Nolta, J.A. (2007). Cytokine and integrin stimulation synergize to promote higher levels of GATA-2, c-Myb, and CD34 protein in primary human hematopoietic progenitors from bone marrow. Blood 109, 2373–2379.

Gaspar, H.B., Bjorkegren, E., Parsley, K., Gilmour, K.C., King, D., Sinclair, J., Zhang, F., Giannakopoulos, A., Adams, S., Fairbanks, LD., Gaspar, J., Henderson, L., Xu-Bayford, J.H., Davies, E.G., Veys, P.A., Kinnon, C., and Thrasher, A.J. (2006). Successful reconstitution of immunity in ADA-SCID by stem cell gene therapy following cessation of PEG-ADA and use of mild preconditioning. Mol. Ther. 14, 505–513.

Hanenberg, H., Xiao, X.L., Dilloo, D., Hashino, K., Kato, I., and Williams, D.A. (1996). Colocalization of retrovirus and target cells on specific fibronectin fragments increases genetic transduction of mammalian cells. Nat. Med. 2, 876–882.

Hanenberg, H., Hashino, K., Konishi, H., Hock, R.A., Kato, I., and Williams, D.A. (1997). Optimization of fibronectin-assisted retroviral gene transfer into human CD34$^+$ hematopoietic cells. Hum. Gene Ther. 8, 2193–2206.

Kimizuka, F., Taguchi, Y., Ohdate, Y., Kawase, Y., Shimojo, T., Hashino, K., Kato, I., Sekiguchi, K., and Titani, K. (1991). Production and characterization of functional domains of human fibronectin expressed in *Escherichia coli*. J. Biochem. 110, 284–291.

Kiyokawa, N., Kokai, Y., Ishimoto, K., Fujita, H., Fujimoto, J., and Hata, J. (1990). Characterization of the common acute lymphoblastic leukemia antigen (CD10) as an activation molecule on mature human B cells. Clin. Exp. Immunol. 79, 322–327.

Murray, L., Luens, K., Tushinski, R., Jin, L., Burton, M., Chen, J., Forestell, S., and Hill, B. (1999). Optimization of retroviral gene transduction of mobilized primitive hematopoietic progenitors by using thrombopoietin, Flt3, and Kit ligands and RetroNectin culture. Hum. Gene Ther. 10, 1743–1752.

Onodera, M., Ariga, T., Kawamura, N., Kobayashi, I., Ohtsu, M., Yamada, M., Tame, A., Furuta, H., Okano, M., Matsumoto, S., Kotani, H., McGarrity, G.J., Blaese, R.M., and Sakiyama, Y. (1998). Successful peripheral T-lymphocyte-directed gene transfer for a patient with severe combined immune deficiency caused by adenosine deaminase deficiency. Blood 91, 30–36.

Ott, M.G., Schmidt, M., Schwarzwaelder, K., Stein, S., Siler, U., Koehl, U., Glimm, H., Kulcke, K., Schilz, A., Kunkel, H.,

Naundorf, S., Brinkmann, A., Deichmann, A., Fischer, M., Ball, C., Pilz, I., Dunbar, C., Du, Y., Jenkins, N.A., Copeland, N.G., Luhi, U., Hassan, M., Thrasher, A.J., Hoelzer, D., von Kalle, C., Seger, R., and Grez, M. (2006). Correction of X-linked chronic granulomatous disease by gene therapy, augmented by insertional activation of MDS1-EVI1, PRDM16 or SETBP1. Nat. Med. 12, 401–409.

Pellinen, T., and Ivaska, J. (2006). Integrin traffic. J. Cell Sci. 119, 3723–3731.

Suzuki, A., Obi, K., Urabe, T., Hayakawa, H., Yamada, M., Kaneko, S., Onodera, M., Mizuno, Y., and Mochizuki, H. (2002). Feasibility of *ex vivo* gene therapy for neurological disorders using the new retroviral vector GCDNsap packaged in the vesicular stomatitis virus G protein. J. Neurochem. 82, 953–960.

Address correspondence to:
Dr. Nobutaka Kiyokawa
Department of Developmental Biology
National Research Institute for Child Health and Development
2-10-1, Okura, Setagaya-ku
Tokyo 157-8535, Japan

E-mail: nkiyokawa@nch.go.jp

Received for publication September 29, 2008;
accepted after revision March 13, 2009.

Published online: April 9, 2009.

Immunology
The Journal of cells, molecules, systems and technologies
British Society for immunology
IMMUNOLOGY ORIGINAL ARTICLE

Ex vivo expanded cord blood CD4 T lymphocytes exhibit a distinct expression profile of cytokine-related genes from those of peripheral blood origin

Yoshitaka Miyagawa,[1] Nobutaka Kiyokawa,[1] Nakaba Ochiai,[2,3] Ken-Ichi Imadome,[4] Yasuomi Horiuchi,[1] Keiko Onda,[1] Misako Yajima,[4] Hiroyuki Nakamura,[4] Yohko U. Katagiri,[1] Hajime Okita,[1] Tomohiro Morio,[2,5] Norio Shimizu,[2,6] Junichiro Fujimoto[7] and Shigeyoshi Fujiwara,[4]

[1]*Department of Developmental Biology, National Research Institute for Child Health and Development, Setagaya-ku,* [2]*Center for Cell Therapy, Tokyo Medical and Dental University Medical Hospital, Bunkyo-ku, Tokyo,* [3]*Lymphotec Inc., Koto-ku, Tokyo,* [4]*Department of Infectious Diseases, National Research Institute for Child Health and Development, Setagaya-ku, Tokyo,* [5]*Department of Pediatrics and Developmental Biology, Graduate School of Medicine, Tokyo Medical and Dental University, Bunkyo-ku, Tokyo,* [6]*Department of Virology, Division of Medical Science, Medical Research Institute, Tokyo Medical and Dental University, Bunkyo-ku, Tokyo, and* [7]*Vice Director General, National Research Institute for Child Health and Development, Setagaya-ku, Tokyo, Japan*

doi:10.1111/j.1365-2567.2009.03122.x
Received 1 September 2008; revised 30 March 2009; accepted 15 April 2009.
Correspondence: N. Kiyokawa, MD, PhD, Department of Developmental Biology, National Research Institute for Child Health and Development, 2-10-1, Okura, Setagaya-ku, Tokyo 157-8535, Japan.
Email: nkiyokawa@nch.go.jp
Senior author: Nobutaka Kiyokawa

Summary

With an increase in the importance of umbilical cord blood (CB) as an alternative source of haematopoietic progenitors for allogenic transplantation, donor lymphocyte infusion (DLI) with donor CB-derived activated CD4$^+$ T cells in the unrelated CB transplantation setting is expected to be of increased usefulness as a direct approach for improving post-transplant immune function. To clarify the characteristics of activated CD4$^+$ T cells derived from CB, we investigated their mRNA expression profiles and compared them with those of peripheral blood (PB)-derived activated CD4$^+$ T cells. Based on the results of a DNA microarray analysis and quantitative real-time reverse transcriptase–polymerase chain reaction (RT-PCR), a relatively high level of forkhead box protein 3 (Foxp3) gene expression and a relatively low level of interleukin (IL)-17 gene expression were revealed to be significant features of the gene expression profile of CB-derived activated CD4$^+$ T cells. Flow cytometric analysis further revealed protein expression of Foxp3 in a portion of CB-derived activated CD4$^+$ T cells. The low level of retinoic acid receptor-related orphan receptor γ isoform t (RORγt) gene expression in CB-derived activated CD4$^+$ T cells was speculated to be responsible for the low level of IL-17 gene expression. Our data indicate a difference in gene expression between CD4$^+$ T cells from CB and those from PB. The findings of Foxp3 expression, a characteristic of regulatory T cells, and a low level of IL-17 gene expression suggest that CB-derived CD4$^+$ T cells may be a more appropriate source for DLI.

Keywords: CD4; cord blood; donor lymphocyte infusion; forkhead box protein 3; interleukin 17; T cell

Abbreviations: BIM, BCL2-like 11; CB, cord blood; CTLA-4, cytotoxic T-lymphocyte antigen-4; CDKN, cyclin-dependent kinase inhibitor; DLI, donor lymphocyte infusion; Foxp3, forkhead box protein 3; GAPDH, glyceraldehyde-3-phosphate dehydrogenase; GM-CSF, granulocyte–macrophage colony-stimulating factor; GVHD, graft-versus-host disease; GVL, graft-versus-leukaemia; HSCT, haematopoietic stem cell transplantation; ICOS, inducible T-cell co-stimulator; IFNG, interferon γ; IL, interleukin; PB, peripheral blood; RORγt, retinoic acid receptor-related orphan receptor γ isoform t; RT, reverse transcriptase; TCR, T-cell receptor; Th, T helper cell; Treg, regulatory T cell.

© 2009 Blackwell Publishing Ltd,

Introduction

Donor lymphocyte infusion (DLI) is a direct and useful approach for improving post-transplant immune function. DLI has been shown to exert a graft-versus-leukaemia (GVL) effect and has emerged as an effective strategy for the treatment of patients with leukaemia, especially chronic myelogenous leukaemia, who have relapsed after unrelated haematopoietic stem cell transplantation (HSCT).[1] In addition, DLI has been successfully used for some life-threatening viral infections, including Epstein–Barr virus and cytomegalovirus infections after HSCT.[2]

Although DLI frequently results in significant acute and/or chronic graft-versus-host disease (GVHD), several groups have demonstrated that depletion of CD8 T cells from DLIs efficiently reduces the incidence and severity of GVHD while maintaining GVL activity.[3,4] Therefore, selective CD4 DLI is expected to provide an effective and low-toxicity therapeutic strategy for improving post-transplant immune function. Actually, selective CD4 DLI based on a recently established method for *ex vivo* T-cell expansion using anti-CD3 monoclonal antibody and interleukin (IL)-2 is now becoming established as a routine therapeutic means of resolving post-transplant immunological problems in Japan.[5]

The importance of umbilical cord blood (CB) as an alternative source of haematopoietic progenitors for allogenic transplantation, mainly in patients lacking a human leucocyte antigen (HLA)-matched marrow donor, has increased in recent years. Because of the naïve nature of CB lymphocytes, the incidence and severity of GVHD are reduced in comparison with the allogenic transplant setting. In addition, CB is rich in primitive $CD16^{-}$ $CD56^{+}$ natural killer (NK) cells, which possess significant proliferative and cytotoxic capacities, and so have a substantial GVL effect.[6]

In contrast, a major disadvantage of CB transplantation is the low yield of stem cells, resulting in higher rates of engraftment failure and slower engraftment compared with bone marrow transplantation. In addition, it was generally thought to be difficult to perform DLI after CB transplantation using donor peripheral blood (PB), with the exception of transplantations from siblings. However, the above-described method for the *ex vivo* expansion of activated T cells can produce a sufficient amount of cells for therapy using the CB cell residues in an infused bag, which has solved this problem and made it possible to perform DLI with donor CB-derived activated $CD4^{+}$ T cells in the unrelated CB transplantation setting.[5] It has also been reported that CB-derived T cells can be expanded *ex vivo* while retaining the naïve and/or central memory phenotype and polyclonal T-cell receptor (TCR) diversity,[7] and thus potential utilization for adoptive cellular immunotherapy post-CB transplantation has been suggested.[8]

There are functional differences between CB and PB lymphocytes, although the details remain unclear. In an attempt to clarify the differences in characteristics between activated $CD4^{+}$ T cells derived from CB and those derived from PB, we investigated gene expression profiles. In this paper we present evidence that CB-derived $CD4^{+}$ T cells are distinct from PB-derived $CD4^{+}$ T cells in terms of gene expression.

Materials and methods

Cell culture and preparation

CB was distributed by the Tokyo Cord Blood Bank (Tokyo, Japan). The CB was originally collected and stored for stem cell transplantation. Stocks that were inappropriate for transplantation because they contained too few cells were distributed for research use with informed consent, with the permission of the ethics committee of the bank. In addition, all of the experiments in this study using distributed CB were performed with the approval of the local ethics committee. The mononuclear cells were isolated by Ficoll-Paque centrifugation and cultured in the presence of an anti-CD3 monoclonal antibody and interleukin (IL)-2 using TLY Culture Kit 25 (Lymphotec Inc., Tokyo, Japan) as described previously.[5] Although several different methods for T-cell stimulation have been reported, this method is currently being used clinically in Japan. Thus we selected this method in this study. After 14 days of culture, $CD4^{+}$ cells were isolated using a magnetic-activated cell sorting (MACS) system (Miltenyi Biotec, Bergisch Gladbach, Germany) according to the manufacturer's instructions. As a control, mononuclear cells isolated from the peripheral blood of healthy volunteers were similar examined.

Polymerase chain reaction (PCR)

Total RNA was extracted from cells using an RNeasy kit (Qiagen, Valencia, CA) and reverse-transcribed using a First-Strand cDNA synthesis kit (GE Healthcare Bio-Science Corp., Little Chalfont, Buckinghamshire, UK) according to the manufacturer's instructions. Using cDNA synthesized from 150 ng of total RNA as a template for one amplification, real-time reverse transcriptase (RT)-PCR was performed using SYBR® Green PCR master mix, TaqMan® Universal PCR master mix and TaqMan® gene expression assays (Applied Biosystems, Foster City, CA), and an inventoried assay carried out on an ABI PRISM® 7900HT sequence detection system (Applied Biosystems) according to the instructions provided. Either the glyceraldehyde-3-phosphate dehydrogenase (GAP-DH) gene or the β-actin gene was used as an internal control for normalization. The sequences of gene-specific primers for real-time RT-PCR are listed in Table 1.

DNA microarray analysis

The microarray analysis was performed as previously described.[9] Total RNA isolated from cells was reverse-

© 2009 Blackwell Publishing Ltd,

Table 1. The sequences of gene-specific primers for reverse transcriptase–polymerase chain reaction (RT-PCR) and real-time RT-PCR used in this study

Primer	Sequence
IL-4 forward	CACAGGCACAAGCAGCTGAT
IL-4 reverse	CCTTCACAGGACAGGAATTCAAG
IL-6 forward	GTAGCCGCCCCACACAGA
IL-6 reverse	CCGTCGAGGATGTACCGAAT
IL-10 forward	GCCAAGCCTTGTCTGAGATGA
IL-10 reverse	CTTGATGTCTGGGTCTTGGTTCT
IL-17 forward	GACTCCTGGGAAGACCTCATTG
IL-17 reverse	TGTGATTCCTGCCTTCACTATGG
IL-17F forward	GCTTGACATTGGCATCATCAA
IL-17F reverse	GGAGCGGCTCTCGATGTTAC
IL-23 forward	GAGCCTTCTCTGCTCCCTGATAG
IL-23 reverse	AGTTGGCTGAGGCCCAGTAG
IL-23R forward	AACAACAGCTCGGCTTTGGTATA
IL-23R reverse	GGGACATTCAGCAGTGCAGTAC
IFNG forward	CATCCAAGTGATGGCTGAACTG
IFNG reverse	TCGAAACAGCATCTGACTCCTTT
GM-CSF forward	CAGCCCTGGAGCATGTG
GM-CSF reverse	CATCTCAGCAGCAGTGTCTCTAC
RORγt forward	TGGGCATGTCCCGAGATG
RORγt reverse	GCAGGCTGTCCCTCTGCTT
STAT-3 forward	GGAGGAGGCATTCGGAAAGT
STAT-3 reverse	GCGCTACCTGGGTCAGCTT
FOXP3 forward	GAGAAGCTGAGTGCCATGCA
FOXP3 reverse	GCCACAGATGAAGCCTTGGT

IL, interleukin; *IFNG*, interferon γ; *FOXP3*, forkhead box protein 3; *GM-CSF*, granulocyte–macrophage colony-stimulating factor; *RORγt*, retinoic acid receptor-related orphan receptor γ isoform t; *STAT*, signal transducer and activator of transcription.

transcribed and labelled using One-Cycle Target Labeling and Control Reagents as instructed by the manufacturer (Affymetrix, Santa Clara, CA). The labelled probes were hybridized to a Human Genome U133 Plus 2·0 Array (Affymetrix). The arrays were used in a single experiment and analysed with GENECHIP operating software 1.2 (Affymetrix). Background subtraction and normalization were performed using GENESPRING GX 7.3 software (Agilent Technologies, Santa Clara, CA). The signal intensity was pre-normalized based on the positive control genes (GAPDH and β-actin) for all measurements on that chip. To account for differences in detection efficiency between spots, the pre-normalized signal intensity of each gene was normalized to the median of pre-normalized measurements for that gene. The data were filtered as follows. (i) Genes that were scored as absent in all samples were eliminated. (ii) Genes with a signal intensity of < 90 were eliminated. (iii) Genes that exhibited increased (fold-change > 2) or decreased (fold-change > 2) expression in CB-derived CD4$^+$ T cells compared with PB-derived CD4$^+$ T cells were selected by comparing the mean value of signal intensities in each condition.

Immunofluorescence study

After periods of cultivation, cells were collected and stained with fluorescence-labelled monoclonal antibodies and analysed by flow cytometry (FC500; Beckman/Coulter, Fullerton, CA). A four-colour immunofluorescence study was performed with a combination of fluorescein isothiocyanate (FITC)-conjugated anti-CD3, phycoerythrin (PE)-conjugated anti- forkhead box protein 3 (Foxp3), phycoerythrin-cyanine-5 (PC5)-conjugated anti-CD4 and PC7-conjugated anti-CD8 (Beckman/Coulter). After staining of cell surface antigens, cells were permeabilized with IntraPrep (Dako, Glostrup, Denmark) and intracellular antigen (Foxp3) was further stained.

Statistical analysis

The statistical analysis was performed using a Student's *t*-test and a *P*-value < 0·05 was considered to be statistically significant.

Results

Expression profiles of activated CD4$^+$ T cells derived from human CB and PB

To compare the gene expression patterns of CB-derived CD4$^+$ cells and PB-derived CD4$^+$ cells, we performed DNA microarray analysis using the Affymetrix Human Genome U133 Plus 2·0 Array. After background subtraction, comparison of the gene expression profiles of two independent CB-derived CD4$^+$ samples and PB-derived CD4$^+$ samples was performed using a gene cluster analysis. The genes differentially expressed (fold-change > 2) between the activated CD4$^+$ T cells derived from CB and those derived from PB were selected, and 396 probes were found to exhibit higher levels of expression in CB-derived CD4$^+$ samples while 131 probes exhibited higher levels in PB-derived CD4$^+$ samples. Parts of the data are summarized and presented in Fig. 1a and Tables 2–4.

Among these genes, those closely correlated to T-cell function and development were selected (Fig. 1b). The genes exhibiting higher levels of expression in CB-derived CD4$^+$ samples included those encoding cell cycle regulators, including cyclin-dependent kinase (CDKN)2A and 2B, transcriptional regulators and signal transduction factors (Tables 2 and 3). The genes for cytokines, chemokines and their receptors such as Interferon γ (IFNG), granulocyte-macrophage colony-stimulating factor (GM-CSF) and for T-cell transcriptional regulators (*FOXP3*) as well as the genes related to T-cell development including CD28, cytotoxic T lymphocyte antigen-4 (CTLA4) and inducible T-cell co-stimulator (ICOS) were also found among the genes exhibiting higher levels of expression in CB-derived CD4$^+$ samples (Fig. 1b). The factors reported

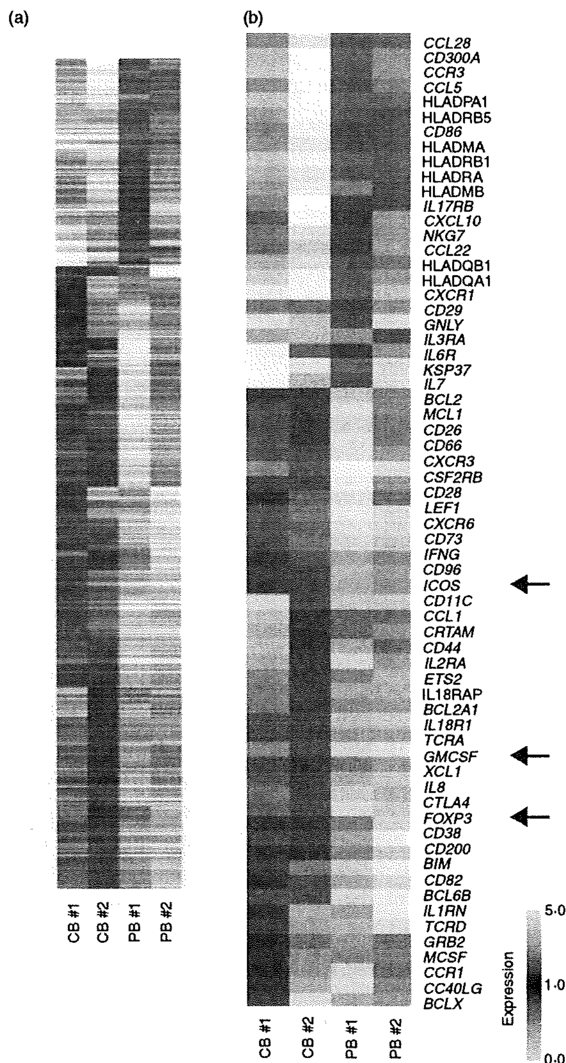

Figure 1. Comparison of the gene expression profiles of cord blood (CB)- and peripheral blood (PB)-derived CD4$^+$ T cells. Hierarchical clustering of results from a microarray analysis for CB- and PB-derived CD4$^+$ T cells is indicated. (a) A total of 529 genes characterizing CD4$^+$ T cells (396 genes for CB-derived CD4$^+$ T cells and 131 genes for PB-derived CD4$^+$ T cells) were used to create the gene tree. The gene list is presented in Tables 3 and 4. (b) Genes related to T-cell development (40 genes for CB-derived CD4$^+$ T cells and 26 genes for PB-derived CD4$^+$ T cells) are presented. The arrows indicate the expression pattern of T-cell lineage-specific genes including inducible T-cell co-stimulator (*ICOS*), granulocyte-macrophage colony-stimulating factor (*GM-CSF*) and forkhead box protein 3 (*FOXP3*).

to be essential for negative selection in CD4$^+$ CD8$^+$ thymocytes such as BCL2-like 11 (BIM)[10] as well as other apoptotic regulators were also found among the genes exhibiting higher expression levels in CB-derived CD4$^+$ samples.

The genes with a higher level of expression in the PB-derived CD4$^+$ T cells included those encoding transcriptional regulators, signal transduction factors, major histocompatibility complex (MHC) class II molecules (*HLADMA*, *HLADMB*, *HLADPA1*, *HLADQB1*, *HLADRA*, *HLADRB1* and *HLADRB5*), and cytokines, chemokines and their receptors (*IL-7*, *IL-17RB*), as well as genes that characterize the T-cell lineage (*CD29*, *CD86*) (Fig. 1b, Tables 2, 4).

Notably, microarray studies showed that the expression of several regulatory T cell (Treg)-related genes was significantly higher in the CB-derived T cells. Foxp3 is an important T-cell transcription factor and is considered to be a marker of Tregs. Cytotoxic T-lymphocyte antigen-4 (CTLA-4) and ICOS, which belong to the CD28 family of receptors and play a crucial role in the activation of T cells, were reported to be highly expressed in activated Tregs.[11,12] All of the above genes were expressed at higher levels in the CB-derived CD4 T cells (Fig. 1).

The microarray results for major genes related to the development of the T-cell lineage, including those not appeared in Fig. 1, are summarized in Table 2. As shown in Table 2, the expression of T-cell lineage master regulator genes, such as *TBX21*, *GATA3* and *MAF*, and T cell-related cytokines, such as *IL-4*, *IL-5*, *IL-13*, *IL-22* and *TGFB1*, revealed no significant difference between CB-derived CD4$^+$ cells and PB-derived CD4$^+$ cells. However, other T cell-related genes, including *IL-2*, *IL-6*, *IL-9*, *IL-10* and *IL-17*, were eliminated from the list in the course of background subtraction because the signal intensity of each gene was low (< 90 as raw data) in all of the samples.

Differences in the expression patterns of T-cell lineage-specific genes between CB-derived and PB-derived CD4$^+$ T cells

To further confirm the characteristic gene expression in CB- and PB-derived CD4$^+$ T cells, we performed a real-time RT-PCR analysis. Consistent with the microarray data, when the mRNA levels of the genes related to the T helper type 1 (Th1) and Th2 phenotypes were examined, higher levels of GM-CSF and IFNG were observed in CB-derived T cells, while IL-4 revealed no significant tendency (Fig. 2). We also examined IL-6 and IL-10 and no significant tendency was observed either in the expression of these genes (Fig. 2).

Next we examined the expression of the genes related to Tregs and observed a higher level of Foxp3, but lower levels of retinoic acid receptor-related orphan receptor γ isoform t (RORγt); and IL-17F, in CB-derived T cells (Fig. 3). In contrast, there was no significant tendency in the expression of genes encoding signal transducer and activator of transcription 3 (STAT-3), IL-23 and IL-23 receptors. In the case of the *IL-17* gene, clear amplifica-

Table 2. The microarray results for T-cell-related genes

Description	Gene	Gene ID	CB-1		CB-2		PB-1		PB-2	
			Normalized	Raw	Normalized	Raw	Normalized	Raw	Normalized	Raw
Master regulation										
Thl	*TBX21*	220684_at	1·1382915	305·7	0·7851455	247·1	1·045663	230·5	0·954337	261·4
Th2	*GATA3*	209602_s_at	1·471558	1204	0·7742825	742·1	1·0740323	721·1	0·9259675	772·5
	GATA3	209603_at	1·265932	416·5	0·53335179	205·7	1·0535141	284·5	0·9464856	317·6
	GATA3	209604_s_at	1·350573	5300	0·6415387	2950	1·0573606	3406	0·9426395	3773
	MAF	206363_at	0·7447395	672·7	0·8744312	925·6	1·1255689	834·5	1·2704437	1170
	MAF	209348_s_at	1·0320604	2078	0·8329663	1965	0·9679398	1600	1·8301903	3758
	MAF	229327_s_at	0·9099149	569·7	0·6089576	446·8	1·090085	560·2	1·4076804	898·9
Treg	*FOXP3*	221334_s_at	1·8893701	100·6	1·4199468	88·6	0·4988136	21·8	0·5800531	31·5
	FOXP3	224211_at	1·6205869	152·3	1·4101433	155·3	0·5898568	45·5	0·2347433	22·5
Cytokines										
Thl	*IFNG*	210354_at	1·4801383	2000	1·9182948	3037	0·457517	507·4	0·5198616	716·4
	GM-CSF	210229_s_at	1·2802086	1293	2·6726868	3163	0·6906437	572·5	0·7197912	741·4
Th2	*IL-4*	207538_at	2·0291064	687·2	0·3361219	133·4	0·9317174	259	1·0682826	369
	IL-4	207539_s_at	2·8263247	965	0·3561467	142·5	0·8481774	237·7	1·1518226	401·1
	IL-5	207952__at	1·3380713	810	0·0610382	43·3	1·0097023	501·7	0·9902797	611·4
	IL-13	207844_at	3·9835246	1712	0·8117443	408·8	1·1453367	404	0·8691162	452·9
Treg	*TGFB1*	203085_s_at	1·5166419	774·9	0·9012154	539·6	1·0987847	460·8	0·8546632	374·6
Others	*IL-22*	222974_at	0·1272062	5·2	4·325279	207·2	0·5632869	18·9	1·4367131	59·9
Surface molecules										
Treg	*CTLA4*	231794_at	1·3871489	336·9	1·2560804	357·5	0·7439196	148·3	0·4444751	110·1
	CTLA4	236341_at	1·2573498	905·7	1·6210791	1368	0·6800935	402·1	0·7426501	545·6
Others	*IL-2RA*	206341_at	1·5216751	3569	1·2715347	3494	0·7284654	1402	0·6569936	1571
	IL-2RA	211269_s_at	1·1563299	4436	1·3173387	5923	0·8436702	2657	0·560745	2194
	ICOS	210439_at	1·378036	619·8	1·343834	708·3	0·567216	209·4	0·656166	301
	CD28	211856_x_at	1·3887135	144·9	1·2905376	157·8	0·3292731	28·2	0·7094624	75·5
	CD28	211861_x_at	1·350062	183·3	1·4109998	224·5	0·4863549	54·2	0·649938	90

The microarray results for major genes related to the development of the T-cell lineage are summarized. The normalized and raw data for four samples are indicated for each gene. Those for which differential expression was found between cord blood (CB)- and peripheral blood (PB)-derived $CD4^+$ T cells in a gene cluster analysis (fold-change > 2) are highlighted in grey. Genes exhibiting low signal intensity (< 90 as raw data) in all of the four samples were eliminated from the list beforehand in the process of background subtraction, and thus do not appeared in this table.

CTLA-4, cytotoxic T-lymphocyte antigen-4; *FOXP3*, forkhead box protein 3; GATA, GATA family of zinc finger trancription factors; *GM-CSF*, granulocyte–macrophage colony-stimulating factor; ICOS, inducible T-cell co-stimulator; IFNG, interferon γ; *IL*, interleukin; MAF, macrophage-activating factor; TBX21, T-box protein 21; TGFB1, transforming growth factor, beta 1; Th1, T helper type 1; Treg, regulatory T cell.

tion was detected in PB-derived T cells whereas no amplification was observed in the samples of CB-derived T cells (data not shown).

To further investigate whether increased expression of the *FOXP3* gene is a general feature of CB-derived $CD4^+$ T cells, we tested four samples of CB-derived $CD4^+$ T cells by real-time RT-PCR analysis and compared the results with those for equivalent numbers of PB-derived samples. As shown in Fig. 4, two CB-derived samples (CB 4 and 5, at 2 weeks) revealed significantly increased gene expression of *FOXP3* when compared with PB-derived samples, whereas the remaining two samples (CB 3 and 6; termed 'additional' samples below) did not. We also tested *FOXP3* gene expression at an earlier time-point in the same samples and observed no significant increase of *FOXP3* gene expression in CB-derived $CD4^+$ T cells at 1 week (Fig. 4). When the data were analysed statistically, expression of the *FOXP3* gene was found to be significantly higher in CB-derived $CD4^+$ T cells in comparison with equivalent PB-derived $CD4^+$ T cells at both 1 week ($P < 0.05$) and 2 weeks ($P < 0.05$) (Fig. 4).

Next we assessed the expression of the Foxp3 protein in CB-derived $CD4^+$ T cells. When the same samples as described above were examined by flow cytometry using a specific antibody, the Foxp3 protein was certainly detected in a portion of cells in all of four CB-derived samples while not detected in any of the PB-derived samples tested (Fig. 5). Inconsistent with the results of real-time RT-PCR, expression level of Foxp3 proteins was higher in CB-derived $CD4^+$ T cells at 1 week than at 2 weeks.

Table 3. Genes up-regulated in CD4+ T cells from cord blood samples 1 and 2 (CB 1 and CB 2, respectively)

Affi ID	Gene abbreviation	Fold change				Gene name
		CB 1	CB 2	PB 1	PB 2	
Apoptosis						
1555372_at	*BimL*	1·39	1·52	0·61	0·42	BCL2-like 11 (apoptosis facilitator)
237837_at	*BCL2*	1·27	1·32	0·49	0·73	B-cell CLL/lymphoma 2
205681_at	*BCL2A1*	1·91	1·53	0·39	0·47	BCL2-related protein A1
1558143_a_at	*BCL2L11*	1·68	1·74	0·32	0·32	BGL2-like 11 (apoptosis facilitator)
228311_at	*BCL6B*	1·36	3·39	0·64	0·26	B-cell CLL/lymphoma 6, member B (zinc finger protein)
215037_s_at	*BCLX*	2·56	1·27	0·73	0·56	BCL2-like 1
224414_s_at	*CARD6*	2·65	1·34	0·56	0·66	Caspase recruitment domain family, member 6
201631_s_at	*IER3*	1·62	2·95	0·38	0·31	Immediate early response 3
218000_s_at	*PHLDA1*	2·34	1·21	0·53	0·79	Pleckstrin homology-like domain, family A, member 1
209803_s_at	*PHLDA2*	2·87	1·32	0·31	0·68	Pleckstrin homology-like domain, family A, member 2
203063_at	*PPMIF*	1·26	1·53	0·74	0·64	Protein phosphatase IF (PP2C domain containing)
205214_at	*STK17B*	1·78	1·26	0·74	0·71	Serine/threonine kinase 17b (apoptosis-inducing)
217853_at	*TENS1*	1·63	6·00	0·04	0·37	Tensin 1
B- and T-cell development						
211861_x_at	*CD28*	1·35	1·41	0·49	0·65	CD28 antigen(Tp44)
207892_at	*CD40LG*	3·67	1·32	0·45	0·68	C040 ligand (TNF superfamily, member 5, hyper-IgM syndrome)
206914_at	*CRTAM*	2·76	1·60	0·40	0·36	Class I MHC-restricted T-cell-associated molecule
210557_x_at	*CSF1*	3·79	1·22	0·78	0·70	Colony-stimulating factor 1 (macrophage)
210229_s_at	*CSF2*	1·28	2·67	0·69	0·72	Colony-stimulating factor 2 (granulocyte–macrophage)
205159_at	*CSF2RB*	2·33	1·60	0·18	0·40	Colony-stimulating factor 2 receptor
231794_at	*CTLA4*	1·39	1·26	0·74	0·44	Cytotoxic T-lymphocyte-associated protein 4
204232_at	*FCER1G*	1·63	2·14	0·28	0·37	Fc fragment of IgE, high affinity 1, receptor for; gamma polypeptide
210439_at	*ICOS*	1·38	1·34	0·57	0·66	Inducible T-cell costimulator
210354_at	*IFNG*	1·48	1·92	0·46	0·52	Human mRNA for HuIFN -gamma interferon
230536_at	*PBX4*	1·48	1·26	0·50	0·74	Pre-B-cell leukaemia transcription factor 4
215540_at	*TCRA*	1·25	1·87	0·67	0·75	T-cell antigen receptor alpha
234440_al	*TCRD*	7·51	1·48	0·50	0·52	Human T-cell receptor delta-chain
Cell growth and maintenance						
213497_at	*ABTB2*	2·06	1·34	0·66	0·63	Ankyrin repeat and BTB (POZ) domain containing 2
201236_s_at	*BTG2*	1·60	1·23	0·60	0·77	BTG family, member 2
235287_at	*CDK6*	1·50	1·32	0·44	0·68	Cyclin-dependent kinase 6
209644_x_at	*CDKN2A*	2·90	1·21	0·67	0·79	Cyclin-dependent kinase inhibitor 2A (melanoma, p16, inhibits CDK4)
236313_at	*CDKN2B*	3·24	1·28	0·58	0·72	Cyclin-dependent kinase inhibitor 2B (p15, inhibits CDK4)
241984_at	*CHES1*	1·38	1·34	0·66	0·63	Checkpoint suppressor 1
202552_s_at	CRIM1	1·94	1·39	0·32	0·61	Cysteine-rich transmembrane BMP regulator 1 (chordin-like)
204844_at	*ENPEP*	1·64	1·75	0·09	0·36	Glutamyl aminopeptidase (aminopeptidase A)
205418_at	*FES*	1·39	1·80	0·61	0·25	Feline sarcoma oncogene
228572_at	*GRB2*	4·69	1·21	0·79	0·78	Growth factor receptor-bound protein 2
207688_s_at	*INHBC*	1·46	1·25	0·51	0·75	Inhibin, beta C
209744_x_at	*ITCH*	1·30	1·47	0·63	0·70	Itchy homolog E3 ubiquitin protein ligase (mouse)
201548_s_at	*JARID1B*	1·27	1·92	0·73	0·46	Jumonji, AT-rich interactive domain IB (RBP2-like)
203297_s_at	*JARID2*	1·42	1·28	0·54	0·72	Jumonji, AT-rich interactive domain 2
41387_r_at	*JMJD3*	1·82	1·24	0·76	0·65	Jumonji domain containing 3
205569_at	*LAMP3*	2·32	1·24	0·76	0·50	Lysosomal-associated membrane protein 3
214039_s_at	*LAPTM4B*	1·41	1·49	0·49	0·59	Lysosomal-associated protein transmembrane 4 beta
205857_x_at	*MSH3*	1·79	1·28	0·58	0·72	MutS homolog 3 (*E. coli*)
209550_at	*NDN*	3·42	1·38	0·17	0·62	Necdin homolog (mouse)
207943_x_at	*PLAGL1*	1·37	1·43	0·57	0·63	Pleiomorphic adenoma gene-like 1
204748_at	*PTGS2*	1·65	1·78	0·14	0·35	Prostaglandin-endoperoxide synthase 2
201482_at	*QSCN6*	1·32	1·23	0·38	0·77	Quiescin Q6
203743_s_at	*TDG*	1·47	1·23	0·54	0·77	Thymine-DNA glycosylase
204227_s_at	*TK2*	2·12	1·26	0·56	0·74	Thymidine kinase 2, mitochondrial

Table 3. Continued

Affi ID	Gene abbreviation	Fold change CB 1	CB 2	PB 1	PB 2	Gene name
Cytokines and chemokines						
207533_at	*CCL1*	1·67	1·48	0·52	0·49	Chemokine (C-C motif) ligand 1
205099_s_at	*CCR1*	4·70	1·21	0·61	0·79	Chemokine (C-C motif) receptor 1
207681_at	*CXCR3*	1·51	1·33	0·41	0·67	Chemokine (C-X-C motif) receptor 3
211469_s_at	*CXCR6*	1·58	1·95	0·32	0·42	Chemokine (C-X-C motif) receptor 6
206613_at	*IL-18R1*	2·32	1·38	0·61	0·62	Interleukin-18 receptor 1
207072_at	*IL-18RAP*	2·16	1·44	0·46	0·56	Interleukin-18 receptor accessory protein
212657_s_at	*IL-1RN*	1·44	3·12	0·56	0·37	Interleukin 1 receptor
206341_at	*IL-2RA*	1·52	1·27	0·73	0·66	Interleukin-2 receptor alpha
202859_x_at	*IL-8*	1·31	3·75	0·38	0·69	Interleukin-8
202643_s_at	*TNFAIP3*	1·61	1·25	0·67	0·75	Tumour necrosis factor, alpha-induced protein 3
202687_s_at	*TNFSF10*	2·83	1·23	0·67	0·77	Tumour necrosis factor (ligand) superfamily member 10
205599_at	*TRAF1*	2·25	1·32	0·68	0·61	Tumour necrosis factor receptor-associated factor 1
202871_at	*TRAF4*	1·43	1·58	0·57	0·48	Tumour necrosis factor receptor-associated factor 4
206366_x_at	*XCL1*	1·24	2·66	0·46	0·76	Chemokine (C motif) ligand 1
Signal transduction						
210538_s_at	*AIP1*	1·35	1·54	0·65	0·61	Baculoviral IAP repeat-containing 3
209369_at	*ANXA3*	1·39	6·82	0·61	0·05	Annexin A3
1554343_a_at	*BRDG1*	1·45	1·67	0·52	0·55	BCR downstream signalling 1
225946_at	*C12orf2*	3·20	1·77	0·23	0·23	Ras association (RalGDS/AF-6) domain family 8
204392_at	*CAMK1*	1·26	1·62	0·74	0·54	Calcium/calmodulin-dependent protein kinase I
231042_s_at	*CAMK2D*	1·31	1·63	0·25	0·69	Calcium/calmodulin-dependent protein kinase (CaM kinase) II delta
205692_s_at	*CD38*	1·37	1·29	0·71	0·48	CD38 antigen (p45)
231747_at	*CYSLTR1*	3·16	1·45	0·55	0·43	Cysteinyl leukotriene receptor 1
211272_s_at	*DGKA*	1·43	1·23	0·77	0·54	Diacylglycerol kinase alpha 80 kDa
200762_at	*DPYSL2*	1·35	1·40	0·37	0·65	Dihydropyrimtdinase-like 2
208370_s_at	*DSCR1*	1·23	1·90	0·63	0·77	Down syndrome critical region gene 1
204794_at	*DUSP2*	1·55	2·57	0·39	0·45	Dual specificity phosphatase 2
204015_s_at	*DUSP4*	1·35	2·66	0·65	0·39	Dual specificity phosphatase 4
211333_s_at	*FASLG*	1·20	1·37	0·49	0·80	Fas ligand (TNF superfamily, member 6)
211535_s_at	*FGFR1*	1·23	2·79	0·70	0·77	Fibroblast growth factor receptor 1
224148_at	*FYB*	1·50	1·21	0·45	0·79	FYN binding protein (FYB-120/130)
209304_x_at	*GADD45B*	1·55	1·29	0·65	0·71	Growth arrest and DNA-damage-inducible beta
234284_at	*GNG8*	1·50	3·16	0·50	0·35	Guanine nucleotide binding protein (G protein), gamma 8
224285_at	*GPR174*	1·91	1·42	0·56	0·58	G protein-coupled receptor 174
223767_at	*GPR84*	4·41	1·44	0·05	0·56	G protein-coupled receptor 84
211555_s_at	*GUCY1B3*	1·66	1·73	0·34	0·03	Guanylate cyclase 1, soluble, beta 3
38037_at	*HBEGF*	1·54	1·36	0·55	0·64	Heparin-binding EGF-like growth factor
203820_s_at	*IMP-3*	1·83	2·18	0·17	0·17	IGF-II-mRNA-binding protein 3
203006_at	*INPP5A*	1·40	1·86	0·60	0·52	Inositol polyphosphate-5-phosphatase, 40 kDa
231779_at	*IRAK2*	1·93	1·46	0·46	0·54	Interleukin-1 receptor associated kinase 2
32137_at	*JAG2*	1·58	1·29	0·71	0·64	Jagged 2
203904_x_at	*KAI1*	1·65	1·59	0·41	0·25	CD82 antigen
235252_at	*KSR*	1·72	1·56	0·43	0·44	Kinase suppressor of ras 1
210948_s_at	*LEF1*	1·21	1·64	0·41	0·79	Hypothetical protein LOC641518
203236_s_at	*LGALS9*	1·48	1·27	0·73	0·51	Lectin, galactoside-binding, soluble, 9 (galectin 9)
220253_s_at	*LRP12*	1·27	1·30	0·31	0·73	Low-density lipoprotein-related protein 12
206637_at	*P2RY14*	1·32	1·48	0·39	0·68	Purinergic receptor P2Y, G-protein coupled, 14
210837_s_at	*PDE4D*	1·35	1·31	0·62	0·69	Phosphodiesterase 4D, cAMP-specific
206726_at	*PGDS*	6·45	1·40	0·60	0·43	Prostaglandin D2 synthase, haematopoietic
210617_at	*PHEX*	1·53	4·08	0·21	0·47	Phosphate regulating endopeptidase homologue, X-linked
206370_at	*PIK3CG*	1·23	1·32	0·50	0·77	Phosphoinositide-3-kinase, catalytic, gamma polypeptide
205632_s_at	*PIP5K1B*	1·32	1·42	0·64	0·68	Phosphalidylinositol-4-phosphate 5-kinase, type 1 beta

Table 3. Continued

Affi ID	Gene abbreviation	Fold change CB 1	CB 2	PB 1	PB 2	Gene name
215195_at	*PRKCA*	2·17	1·36	0·64	0·61	Protein kinase C, alpha
210832_x_at	*PTGER3*	4·44	1·47	0·07	0·53	Prostaglandin E receptor 3 (subtype EP3)
1553535_a_at	*RANGAP1*	1·58	1·39	0·58	0·61	Ran GTPase activating protein 1
234344_at	*RAP2C*	1·75	1·26	0·46	0·74	RAP2C, member of RAS oncogene family
223809_at	*RGS18*	2·12	1·67	0·15	0·33	Regulator of G-protein signalling 18
209882_at	*RIT1*	1·74	1·32	0·63	0·68	Ras-like without CAAX 1
209451_at	*TANK*	1·34	1·20	0·42	0·80	TRAF family member-associated NFKB activator
204924_at	*TLR2*	1·60	2·52	0·36	0·40	Toll-like receptor 2
217979_at	*TM4SF13*	1·21	2·47	0·30	0·79	Tetraspanin 13
209263_x_at	*TM4SF7*	2·05	1·41	0·58	0·59	Tetraspanin 4
Transcription						
1566989_at	*ARID1B*	1·42	1·27	0·09	0·73	AT-rich interactive domain 1B (SWI1-like)
203973_s_at	*CEBPD*	3·06	1·51	0·33	0·49	CCAAT/enhancer binding protein (C/EBP), delta
221598_s_at	*CRSP8*	1·60	1·29	0·71	0·68	Cofactor required for Sp1 transcriptional activation, subunit 8, 34 kDa
205249_at	*EGR2*	1·33	4·27	0·67	0·60	Early growth response 2 (Krox-20 homologue, *Drosophila*)
206115_at	*EGR3*	1·31	6·15	0·69	0·48	Early growth response 3
201328_at	*ETS2*	1·57	1·72	0·43	0·40	V-ets erythroblastosis virus E26 oncogene homologue 2 (avian)
218810_at	*FLJ23231*	2·13	1·37	0·63	0·63	Zinc finger CCCH-type containing 12A
209189_at	*FOS*	21·56	1·31	0·13	0·69	V-fos FBJ murine osteosarcoma viral oncogene homologue
223408_s_at	*FOXK2*	2·26	1·22	0·48	0·78	Forkhead box K2
202723_s_at	*FOXO1A*	1·47	1·27	0·57	0·73	Forkhead box O1A (rhabdomyosarcoma)
224211_at	*FOXP3*	1·62	1·41	0·59	0·23	Forkhead box P3
207156_at	*HIST1H2AG*	1·73	1·30	0·41	0·70	Histone 1, H2ag
220042_x_at	*HIVEP3*	1·26	1·65	0·74	0·56	Human immunodeficiency virus type I enhancer binding protein 3
207826_s_at	*ID3*	1·34	8·64	0·60	0·66	Inhibitor of DNA binding 3, dominant negative helix-loop-hetix protein
204549_at	*IKBKE*	2·33	1·29	0·71	0·66	Inhibitor of kappa light polypeptide gene enhancer in B cells
219878_s_at	*KLF13*	1·89	1·26	0·34	0·74	Kruppel-like factor 13
207667_s_at	*MAP2K3*	1·33	1·28	0·72	0·57	Mitogen-activated protein kinase kinase 3
201502_s_at	*NFKBIA*	2·31	1·29	0·71	0·57	Nuclear factor of κ light polypeptide gene enhancer in B cells inhibitor
222105_s_at	*NKIRAS2*	1·84	1·21	0·69	0·79	NFKB inhibitor interacting Ras-like 2
204622_x_at	*NR4A2*	1·35	4·31	0·65	0·63	Nuclear receptor subfamily 4, group A, member 2
207978_s_at	*NR4A3*	1·33	3·53	0·62	0·67	Nuclear receptor subfamily 4, group A, member 3
202600_s_at	*NRIP1*	1·86	1·39	0·26	0·61	Nuclear receptor interacting protein 1
216841_s_at	*SOD2*	1·25	1·73	0·36	0·75	Superoxide dismutase 2, mitochondrial
201416_at	*SOX4*	1·53	2·21	0·47	0·38	SRY (sex determining region Y)-box 4
223635_s_at	*SSBP3*	2·12	1·25	0·75	0·62	Single-stranded DNA binding protein 3
206506_s_at	*SUPT3H*	1·47	1·31	0·57	0·69	Suppressor of Ty 3 homologue (*S. cerevisiae*)
221618_s_at	*TAF9L*	1·25	1·49	0·47	0·75	TAF9-like RNA polymerase II
203177_x_at	*TFAM*	1·63	1·23	0·77	0·57	Transcription factor A, mitochondrial
213943_at	*TWIST1*	1·89	3·14	0·04	0·11	Twist homologue 1 (acrocephalosyndactyly 3; Saethre-Chotzen syndrome)
219836_at	*ZBED2*	1·33	4·76	0·67	0·21	Zinc finger, BED-type containing 2
211965_at	*ZFP36L1*	2·02	1·47	0·29	0·53	Zinc finger protein 36, C3H type-like 1
230760_at	*ZFY*	1·41	1·25	0·75	0·02	Zinc finger protein, Y-linked
228854_at	*ZNF145*	3·26	1·21	0·40	0·79	Transcribed locus
235121_at	*ZNF542*	2·68	1·33	0·63	0·67	Zinc finger protein 542

To investigate whether increased expression of the *IL-17* gene is a general feature of PB-derived $CD4^+$ T cells, we also tested *IL-17* gene expression in the above-described additional samples by real-time RT-PCR analysis. As shown in Fig. 6, all of four PB-derived $CD4^+$ T-cell samples revealed significantly increased gene expression of *IL-17* when compared with the CB-derived samples at 1 week. At 2 weeks, however, *IL-17* gene expression in PB-derived $CD4^+$ T cells was diminished while some of the CB-derived $CD4^+$ T cells (such as sample CB 4) exhibited increased *IL-17* gene expression. When the data were analysed statistically, expression of the *IL-17* gene was found to be

© 2009 Blackwell Publishing Ltd,

Table 4. Genes up-regulated in $CD4^+$ T cells from peripheral blood (PB)

Affi ID	Gene abbreviation	Fold change CB 1	CB 2	PB 1	PB 2	Gene name
Apoptosis						
1553681_a_at	*PRF1*	0·66	0·51	1·41	1·34	Perforin 1 (pore-forming protein)
B- and T-cell development						
224499_s_at	*AICDA*	0·06	0·44	1·56	3·47	Activation-induced cytidine deaminase
205495_s_at	*GNLY*	0·40	0·51	1·49	6·34	Granulysin
217478_s_at	*HLA-DMA*	0·67	0·39	1·33	1·35	Major histocompatibility complex, class II, DM alpha
203932_at	*HLA-DMB*	0·64	0·31	2·02	1·36	Major histocompatibility complex, class II, DM beta
211991_s_at	*HLA-DPA1*	0·50	0·14	1·54	1·50	Major histocompatibility complex, class II, DP alpha 1
212671_s_at	*HLA-DQA1*	0·44	0·23	1·56	2·56	Major histocompatibility complex, class II, DQ alpha 1
211656_x_at	*HLA-DQB1*	0·63	0·48	1·37	7·07	Major histocompatibility complex, class II, DQ beta 1
210982_s_at	*HLA-DRA*	0·58	0·37	1·50	1·42	Major histocompatibility complex, class II, DR alpha
208306_x_at	*HLA-DRB1*	0·51	0·24	1·49	1·61	Major histocompatibility complex, class II, DR beta 3
204670_x_at	*HLA-DRB5*	0·63	0·22	1·47	1·37	Major histocompatibility complex, class II, DR beta 5
211634_x_at	*IGHV1-69*	0·69	0·77	1·23	1·99	Immunoglobulin heavy variable 1–69
211645_x_at	*IgK*	0·15	0·49	1·51	6·62	Immunoglobulin kappa light chain (IGKV)
221651_x_at	*IGKC*	0·46	0·68	1·32	5·57	Immunoglobulin kappa constant
215379_x_at	*IGLC2*	0·62	0·41	1·38	4·26	Immunoglobulin lambda joining 2
209031_at	*IGSF4*	0·50	0·03	2·33	1·50	Immunoglobulin superfamily, member 4
205686_s_at	*CD86*	0·70	0·23	1·30	1·39	CD86 antigen (CD28 antigen ligand 2, B7-2 antigen)
204698_at	*ISG20*	0·68	0·49	1·32	1·64	Interferon stimulated exonuclease gene, 20 kDa
213915_at	*NKG7*	0·72	0·42	1·28	2·31	Natural killer cell group 7 sequence
Cell growth and maintenance						
201334_s_at	*ARHGEF12*	0·74	0·50	1·26	1·96	Rho guanine nucleotide exchange factor (GEF) 12
230292_at	*CHC1L*	0·70	0·56	1·30	2·02	Regulator of chromosome condensation (RCC1)
205081_at	*CRIP1*	0·56	0·73	1·27	1·75	Cysteine-rich protein 1 (intestinal)
31874_at	*GAS2L1*	0·77	0·52	1·23	2·35	Growth arrest-specific 2 like 1
202364_at	*MXI1*	0·43	0·73	1·27	1·44	MAX interactor 1
219304_s_at	*PDGFD*	0·65	0·71	1·29	3·68	Platelet-derived growth factor D
213397_x_at	*RNASE4*	0·64	0·46	1·36	2·21	Ribonuclease, RNase A family, 4
213566_at	*RNASE6*	0·69	0·39	1·49	1·31	Ribonuclease, RNase A family, k6
219077_s_at	*WWOX*	0·40	0·78	1·25	1·22	WW domain containing oxidoreductase
Cytokine and chemokine						
207861_at	*CCL22*	0·76	0·52	1·24	2·47	Chemokine (C–C motif) ligand 22
238750_at	*CCL28*	0·74	0·45	1·26	1·41	Chemokine (C–C motif) ligand 28
1555759_a_at	*CCL5*	0·71	0·23	1·29	1·92	Chemokine (C–C motif) ligand 5
208304_at	*CCR3*	0·50	0·12	1·50	2·35	Chemokine (C–C motif) receptor 3
205898_at	*CX3CR1*	0·30	0·20	1·70	4·16	Chemokine (C–X3–C motif) receptor 1
204533_at	*CXCL10*	0·80	0·16	1·20	2·53	Chemokine (C–X–C motif) ligand 10
219255_x_at	*IL-17RB*	0·73	0·04	1·27	1·29	Interleukin 17 receptor B
206148_at	*IL-3RA*	0·60	0·54	2·46	1·40	Interleukin 3 receptor, alpha (low affinity)
226333_at	*IL-6R*	0·22	0·79	1·21	2·43	Interleukin-6 receptor
206693_at	*IL-7*	0·09	0·54	1·46	5·86	Interleukin-7
Signal transduction						
204497_at	*ADCY9*	0·76	0·40	1·24	2·40	Adenylate cyclase 9
206170_at	*ADRB2*	0·58	0·35	1·42	3·97	Adrenergic, beta-2-, receptor, surface
202096_s_at	*BZRP*	0·50	0·54	1·59	1·46	Benzodiazapine receptor (peripheral)
230464_at	*EDG8*	0·04	0·09	1·91	2·42	Endothelial differentiation, sphingolipid G-protein-coupled receptor 8
223423_at	*GPR160*	0·54	0·68	1·40	1·32	G protein-coupled receptor 160
227769_at	*GPR27*	0·07	0·08	1·92	244	G protein in-coupled receptor 27
210095_s_at	*IGFBP3*	0·27	0·20	1·73	5·25	Insulin-like growth factor binding protein 3
38671_at	*PLXND1*	0·08	0·65	1·35	2·57	Plexin D1
226101_at	*PRKCE*	0·56	0·43	1·72	1·44	Protein kinase C, epsilon
232629_at	*PROK2*	0·01	0·13	1·87	2·09	Prokineticin 2

Table 4. Continued

Affi ID	Gene abbreviation	Fold change CB 1	CB 2	PB 1	PB 2	Gene name
203329_at	*PTPRM*	0·36	0·62	1·38	1·93	Protein tyrosine phosphatase, receptor type, M
204731_at	*TGFBR3*	0·78	0·55	1·22	2·04	Transforming growth factor, beta receptor III (betaglycan, 300 kDa)
Transcription						
203129_s_at	*KIF5C*	0·67	0·09	1·33	3·43	Kinesin family member 5C
213906_at	*MYBL1*	0·75	0·51	1·25	3·63	V-myb myeloblastosis viral oncogene homologue (avian)-like 1
209815_at	*PTCH*	0·59	0·27	1·41	4·17	Patched homologue (*Drosophila*)
213891_s_at	*TCF4*	0·74	0·65	2·06	1·26	Transcription factor 4
238520_at	*TRERF1*	0·70	0·77	1·23	2·30	Transcriptional regulating factor 1
203603_s_at	*ZFHX1B*	0·74	0·61	1·26	3·63	Zinc finger homobox 1b
213218_at	*ZNF187*	0·74	0·69	1·26	1·76	Zinc finger protein 187
221123_x_at	*ZNF395*	0·38	0·71	1·63	1·29	Zinc finger protein 395

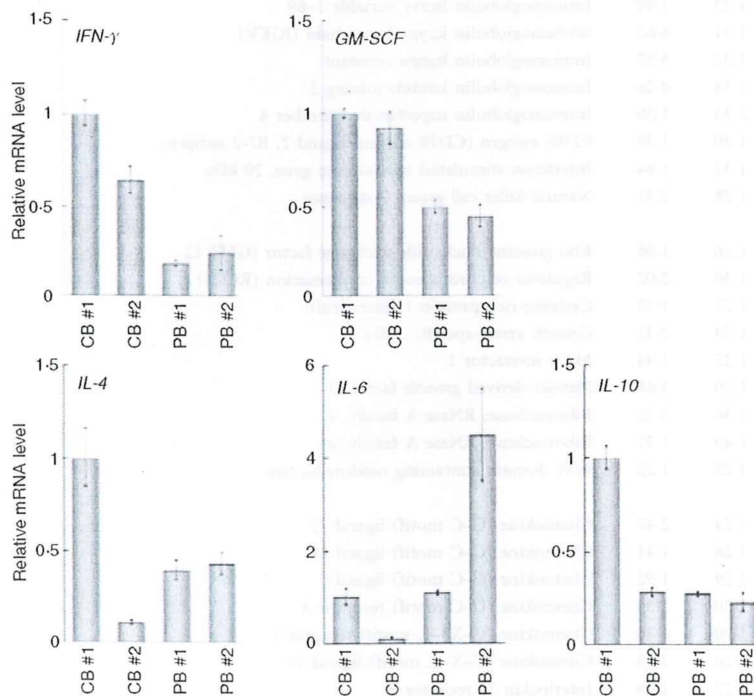

Figure 2. Quantitative polymerase chain reaction (PCR) analysis of the genes related to the T helper type 1 (Th1) and Th2 phenotypes. The expression of the genes indicated was examined by real-time reverse transcriptase (RT)-PCR using the same sample specimens as in Fig 1. Data are normalized to the mRNA level in PB 1 which is arbitrarily set to 1. The signal intensity was normalized using that of a control housekeeping gene [the human glyceraldehyde-3-phosphate dehydrogenase (*GAPDH*) gene]. Data are relative values with the standard deviation (SD) for triplicate wells.

significantly higher in PB-derived $CD4^+$ T cells in comparison with equivalent CB-derived $CD4^+$ T cells at 1 week ($P < 0{\cdot}05$) but not at 2 weeks (Fig. 6).

Discussion

Although it is generally believed that there are functional differences between CB and PB lymphocytes, the details are obscure. For instance, Azuma *et al.*[13] reported that the phenotype and function of expanded CB lymphocytes were essentially equivalent to those of expanded PB lymphocytes when evaluated in *in vitro* experiments. In the present study, however, we have shown that CB-derived $CD4^+$ T cells revealed a distinct expression profile of genes important for the function of particular T-cell subsets compared with PB-derived $CD4^+$ T cells.

$CD4^+$ T cells can be classified into distinct subsets, including effector $CD4^+$ cells and Tregs, according to their functional characteristics as well as differentiation profiles.[14–16] Typically, effector $CD4^+$ T cells have been further divided into two distinct lineages on the basis of their cytokine production profiles, namely Th1 and Th2. Th1 cells producing cytokines such as IL-2, IFN-γ and GM-CSF have evolved to enhance the eradication of intracellular pathogens and are thought to be potent activators of cell-mediated immunity. In contrast, Th2

 © 2009 Blackwell Publishing Ltd,

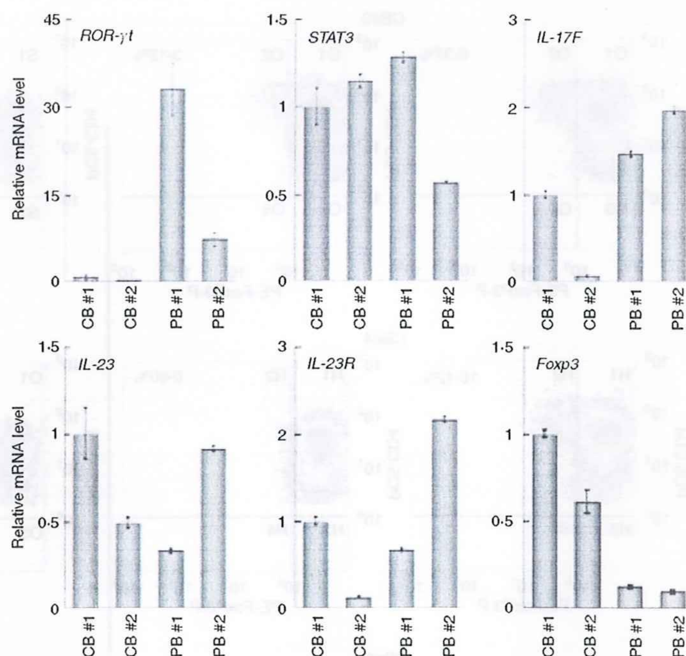

Figure 3. Quantitative polymerase chain reaction (PCR) analysis of the forkhead box protein 3 gene (*FOXP3*) and the genes related to the secretion of interleukin (IL)-17. The expression of the genes indicated was examined as in Fig 2. Data are normalized to the mRNA level in peripheral blood sample 1 (PB 1) as in Fig.2. The signal intensity was normalized using that of a control housekeeping gene [the human glyceraldehyde-3-phosphate dehydrogenase (*GAPDH*) gene]. Data are relative values with the standard deviation for triplicate wells.

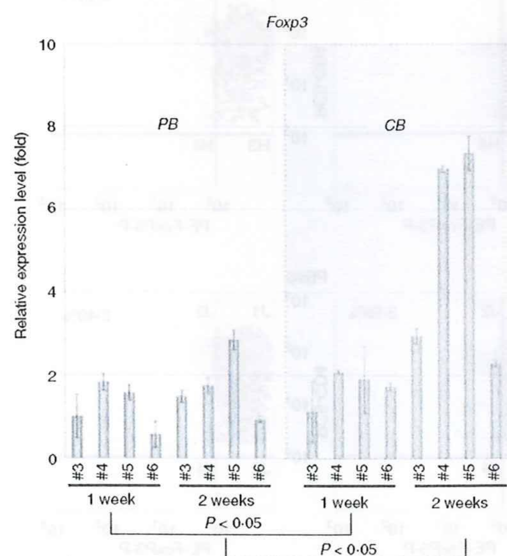

Figure 4. Quantitative polymerase chain reaction (PCR) analysis of the forkhead box protein 3 gene (*FOXP3*) in additional samples. Additional peripheral blood (PB) and cord blood (CB) samples were prepared and RNAs were extracted at 1 and 2 weeks. The expression of the *FOXP3* gene was examined as in Fig. 2. Data are normalized to the mRNA level in the sample of PB 3 at 1 week, which is arbitrarily set to 1. The signal intensity was normalized using that of a control housekeeping gene (the human β-actin gene). Data are relative values with the standard deviation for triplicate wells. The data were analysed statistically and *FOXP3* gene expression in CB-derived $CD4^+$ T cells was found to be significantly higher in comparison with equivalent PB-derived $CD4^+$ T cells at both 1 week ($P < 0{\cdot}05$) and 2 weeks ($P < 0{\cdot}05$).

cells secreting cytokines such as IL-4, IL-5, IL-6, IL-9 and IL-13 have evolved to enhance the elimination of parasitic infections and are thought to be potent activators of B-cell immunoglobulin E production, eosinophil recruitment, and mucosal expulsion. Th1-type responses to self or commensal floral antigens can promote tissue destruction and chronic inflammation, whereas dysregulated Th2-type responses can cause allergy and asthma. The development of Th1 is specified by the transcription factor T-bet (also known as Tbx-21) and master regulators of Th2 differentiation are GATA-3 and c-maf.

As shown in Fig. 2 and Table 2, the gene expression profiles of CB- and PB-derived $CD4^+$ T cells revealed no significant differences regarding cytokines related to the definition of Th1 and Th2, with the exceptions of IFN-γ and GM-CSF. The mRNA levels of IFN-γ and GM-CSF tended to be higher in CB-derived $CD4^+$ T cells than in PB-derived $CD4^+$ T cells. The mRNA expression of the transcription factors T-bet, GATA-3 and c-maf, which regulate Th1 and Th2 cell differentiation, did not differ significantly between CB- and PB-derived $CD4^+$ T cells.

In addition to Th1 and Th2 cells, IL-17 (also known as IL-17A)-producing T lymphocytes have been recently shown to comprise a distinct third subset of T helper cells, termed Th17 cells, in the mouse immune system. Th17 cells exhibit pro-inflammatory characteristics and act as major contributors to autoimmune disease. A number of experiments using animal models support a significant role for IL-17 in the response to allografts.[14,16,17] There is as yet no direct evidence for the existence of discrete Th17 cells in humans, although

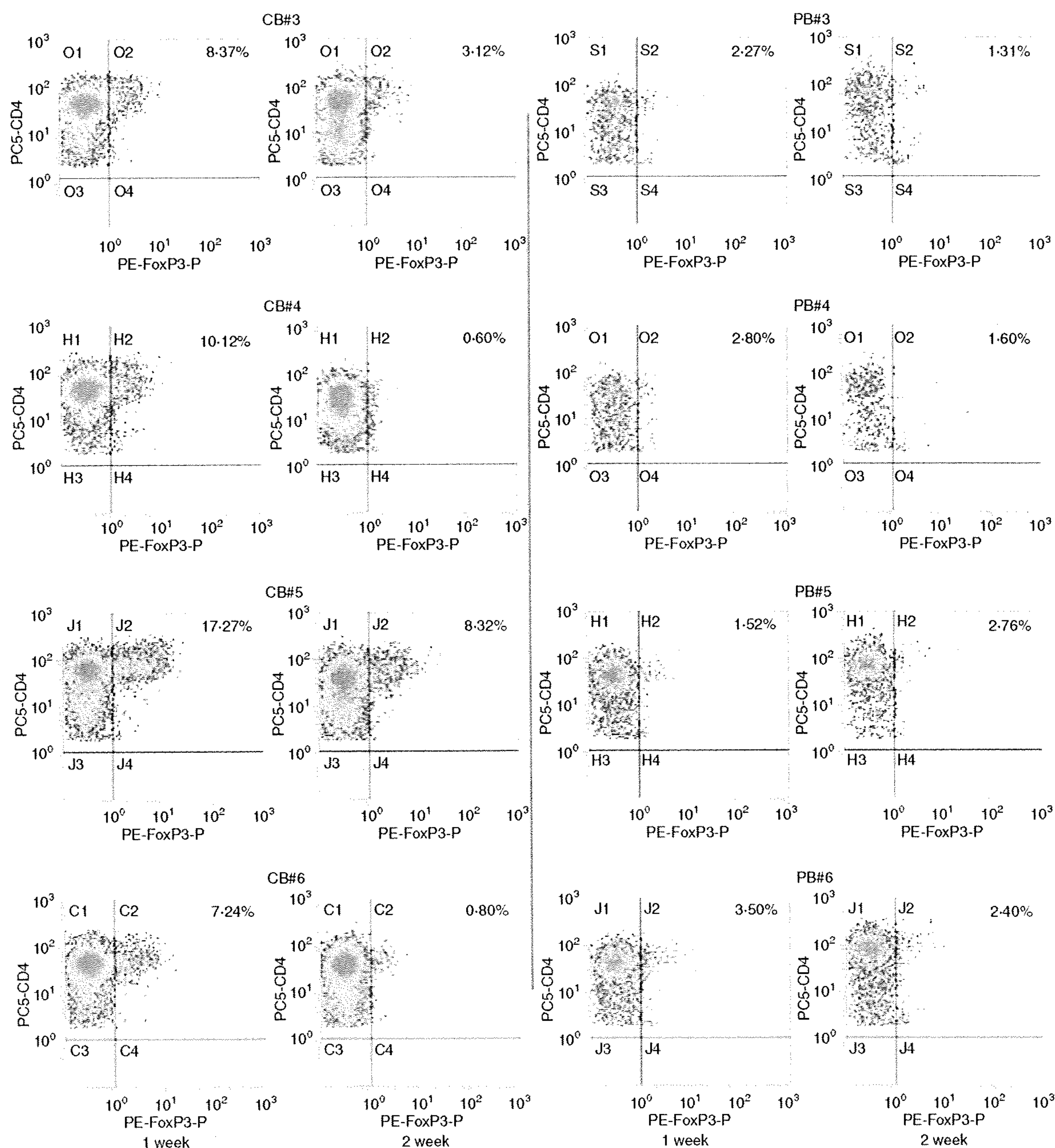

Figure 5. Protein expression of forkhead box protein 3 (Foxp3) in activated CD4+ T cells. The protein expression of Foxp3 in same sample specimens as in Fig. 4 was examined by flow cytometry. The CD4 versus Foxp3 cytogram of the population gated with CD3+ and CD4+ in each sample is presented.

helper T cells secreting IL-17 have clearly been detected in the human immune system.[18] Several studies have shown a correlation between allograft rejection and IL-17. For example, IL-17 levels are elevated in human renal allografts during subclinical rejection and there are detectable mRNA levels in the urinary mononuclear cell sediments of these patients.[19,20] In human lung organ transplantation, IL-17 levels have also been reported to be elevated during acute rejection.[21] Interestingly, in this study, most of the PB-derived CD4+ T-cell samples expressed higher levels of IL-17 mRNA than the CB-derived CD4+ T-cell samples, suggesting that PB-derived CD4+ T cells frequently include potent IL-17-secreting T cells.

 © 2009 Blackwell Publishing Ltd, *Immunology*, **128**, 405–419

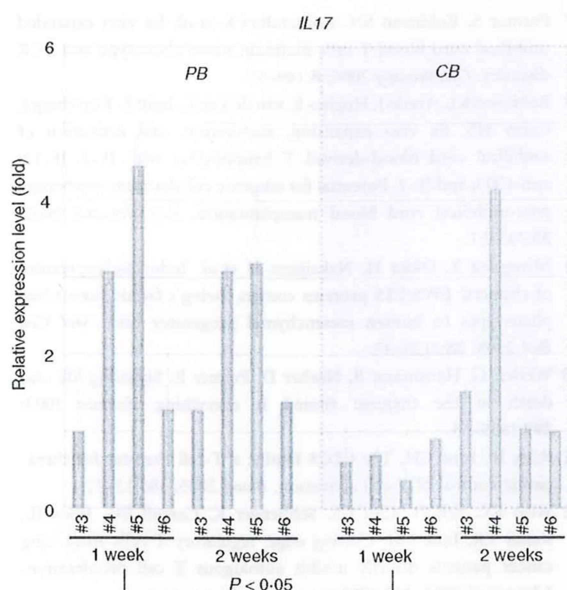

Figure 6. Quantitative polymerase chain reaction (PCR) analysis of interleukin (IL)-17 in additional samples. The expression of the *IL-17* gene in the same sample specimens as in Fig. 4 was examined and presented as in Fig 2. The data were analysed statistically and *IL-17* gene expression in peripheral blood (PB)-derived $CD4^+$ T cells was found to be significantly higher in comparison with equivalent CB-derived $CD4^+$ T cells at 1 week ($P < 0{\cdot}05$) but not at 2 weeks.

Th17 cells expand independently of T-bet or STAT-1. Ivanov *et al.*[22] have shown that the orphan nuclear receptor RORγt is the key transcription factor orchestrating the differentiation of the effector lineage. RORγt induces transcription of the gene encoding IL-17 in naïve $CD4^+$ T helper cells and is required for its expression in response to IL-6 and transforming growth factor (TGF)-β, the cytokines known to induce IL-17 expression. IL-23 is also involved in Th17 cell differentiation, but naïve T cells do not have the IL-23 receptor and are relatively refractory to IL-23 stimulation.[23,24] Although IL-23 seems to be an essential survival factor for Th17 cells, it is not required during their differentiation. It has been suggested that IL-23R expression is up-regulated on RORγt$^+$ Th17 cells in an IL-6-dependent manner. IL-23 may therefore function subsequent to IL-6/TGF-β-induced commitment to the Th17 lineage to promote cell survival and expansion and, potentially, the continued expression of IL-17 and other cytokines that characterize the Th17 phenotype. As presented in Fig. 3, the expression of the *RORγt* gene was significantly weaker in CB-derived $CD4^+$ T cells, whereas the expression of genes encoding IL-23 and the IL-23 receptor did not differ significantly between the $CD4^+$ T cells. Based on the above findings of others, it is possible that the low-level expression of the *RORγt* gene in CB-derived $CD4^+$ T cells is responsible for the absence of *IL-17* mRNA expression in those cells.

Tregs are another functional subset of T cells having anti-inflammatory properties and can cause quiescence of autoimmune diseases and prolongation of transplant function. *In vitro*, Tregs have the ability to inhibit the proliferation and production of cytokines by responder ($CD4^+$ $CD25^-$ and $CD8^+$) T cells subjected to polyclonal stimuli, as well as to down-regulate the responses of $CD8^+$ T cells, NK cells and $CD4^+$ cells to specific antigens.[25,26] These predicates translate *in vivo* to a great number of functions other than the maintenance of tolerance to self-components (prevention of autoimmune disease), such as the ability to prevent transplant rejection. Indeed, donor-specific Tregs can prevent allograft rejection in some models of murine transplant tolerance through a predominant effect on indirect alloresponses.

Foxp3 is thought to be responsible for the development of the Treg population and can act as a phenotypic marker of this fraction.[27] Tregs constitutively express CTLA-4 and there are suggestions that signalling through this pathway may be important for their function, as antibodies to CTLA-4 can inhibit Treg-mediated suppression.[28] As shown above, most of the CB-derived $CD4^+$ T cells were found to express either the *FOXP3* gene or the Foxp3 protein at higher levels compared with PB-derived $CD4^+$ T cells, suggesting that CB-derived $CD4^+$ T cells frequently include a potent Treg population.

As described above, *IL-17* mRNA was more detectable in PB-derived $CD4^+$ cells while *FOXP3* mRNA expression was higher in CB-derived $CD4^+$ cells. Post-transcriptional regulation, as well as differences in mRNA and protein turnover rates, can cause discrepancies between mRNA and protein expression and thus the differences observed in the mRNA expression do not necessary directly indicate those in protein expression.[29] Indeed, we observed some discrepancy between the levels of mRNA and protein with regard to Foxp3 expression in CB-derived $CD4^+$ T cells, as presented above. Nevertheless, changes in mRNA expression are mediated by the alteration of transcriptional regulation, and thus should indicate the differentiation ability of the cells. Therefore, our data indicate that CB-derived $CD4^+$ T cells tend frequently to include potent Tregs, while PB-derived $CD4^+$ T cells tend to include potent IL-17-secreting cells. As described above, DLI with donor CB-derived activated $CD4^+$ T cells is currently becoming established as a routine therapeutic strategy in Japan. It has been proposed that the skewing of responses towards Th17 or Th1 cells and away from Tregs may be responsible for the development and/or progression of autoimmune diseases or acute transplant rejection, and it may thus also be speculated that CB-derived $CD4^+$ T cells are more appropriate for DLI than PB-derived $CD4^+$ T cells.

However, our data also indicate the presence of individual, donor-dependent variations in the characteristics of activated $CD4^+$ T cells derived from CB and PB. More-

over, activated $CD4^+$ T cells do not consist of a single population and should include several distinct functional subsets of $CD4^+$ T cells. Therefore, it is important to clarify the characteristics of activated $CD4^+$ T cells in each preparation to predict the therapeutic effect of DLI in each clinical case.

In summary, our findings demonstrate a difference in gene expression between activated $CD4^+$ T cells derived from CB and those derived from PB. The higher level of *FOXP3* gene expression and the lower level of *IL-17* gene expression in CB-derived $CD4^+$ T cells may indicate that these cells have potential as immunomodulators in DLI therapy. Further detailed analysis should reveal the advantages of activated $CD4^+$ T cells from CB in DLI.

Acknowledgements

We thank the Tokyo Cord Blood Bank for the distribution of cord blood for research use. This work was supported by a grant from the Japan Health Sciences Foundation for Research on Publicly Essential Drugs and Medical Devices (KHC2032), Health and Labour Sciences Research Grants (the 3rd term comprehensive 10-year strategy for cancer control H19-010, Research on Children and Families H18-005, Research on Human Genome Tailor-made and Research on Publicly Essential Drugs and Medical Devices H18-005), and a Grant for Child Health and Development from the Ministry of Health, Labour and Welfare of Japan. It was also supported by CREST, JST.

Disclosures

No competing personal or financial interests exist for any of the authors in relation to this manuscript.

References

1 Loren AW, Porter DL. Donor leukocyte infusions after unrelated donor hematopoietic stem cell transplantation. *Curr Opin Oncol* 2006; **18**:107–14.

2 Roush KS, Hillyer CD. Donor lymphocyte infusion therapy. *Transfus Med Rev* 2002; **16**:161–76.

3 Alyea EP, Soiffer RJ, Canning C *et al.* Toxicity and efficacy of defined doses of CD4(+) donor lymphocytes for treatment of relapse after allogeneic bone marrow transplant. *Blood* 1998; **91**:3671–80.

4 Giralt S, Hester J, Huh Y *et al.* CD8-depleted donor lymphocyte infusion as treatment for relapsed chronic myelogenous leukemia after allogeneic bone marrow transplantation. *Blood* 1995; **86**:4337–43.

5 Tomizawa D, Aoki Y, Nagasawa M *et al.* Novel adopted immunotherapy for mixed chimerism after unrelated cord blood transplantation in Omenn syndrome. *Eur J Haematol* 2005; **75**:441–4.

6 Cohena Y, Nagler A. Hematopoietic stem-cell transplantation using umbilical-cord blood. *Leuk Lymphoma* 2003; **44**:1287–99.

7 Parmar S, Robinson SN, Komanduri K *et al.* Ex vivo expanded umbilical cord blood T cells maintain naive phenotype and TCR diversity. *Cytotherapy* 2006; **8**:149–57.

8 Robinson KL, Ayello J, Hughes R, van de Ven C, Issitt L, Kurtzberg J, Cairo MS. Ex vivo expansion, maturation, and activation of umbilical cord blood-derived T lymphocytes with IL-2, IL-12, anti-CD3, and IL-7. Potential for adoptive cellular immunotherapy post-umbilical cord blood transplantation. *Exp Hematol* 2002; **30**:245–51.

9 Miyagawa Y, Okita H, Nakaijima H *et al.* Inducible expression of chimeric EWS/ETS proteins confers Ewing's family tumor-like phenotypes to human mesenchymal progenitor cells. *Mol Cell Biol* 2008; **28**:2125–37.

10 Werlen G, Hausmann B, Naeher D, Palmer E. Signaling life and death in the thymus: timing is everything. *Science* 2003; **299**:1859–63.

11 Riley JL, June CH. The CD28 family: a T-cell rheostat for therapeutic control of T-cell activation. *Blood* 2005; **105**:13–21.

12 Woo EY, Yeh H, Chu CS, Schlienger K, Carroll RG, Riley JL, Kaiser LR, June CH. Cutting edge: regulatory T cells from lung cancer patients directly inhibit autologous T cell proliferation. *J Immunol* 2002; **168**:4272–6.

13 Azuma H, Yamada Y, Shibuya-Fujiwara N *et al.* Functional evaluation of ex vivo expanded cord blood lymphocytes: possible use for adoptive cellular immunotherapy. *Exp Hematol* 2002; **30**:346–51.

14 Afzali B, Lombardi G, Lechler RI, Lord GM. The role of T helper 17 (Th17) and regulatory T cells (Treg) in human organ transplantation and autoimmune disease. *Clin Exp Immunol* 2007; **148**:32–46.

15 Castellino F, Germain RN. Cooperation between CD4+ and CD8+ T cells: when, where, and how. *Annu Rev Immunol* 2006; **24**:519–40.

16 Reiner SL. Development in motion: helper T cells at work. *Cell* 2007; **129**:33–6.

17 Bi Y, Liu G, Yang R. Th17 cell induction and immune regulatory effects. *J Cell Physiol* 2007; **211**:273–8.

18 Fossiez F, Djossou O, Chomarat P *et al.* T cell interleukin-17 induces stromal cells to produce proinflammatory and hematopoietic cytokines. *J Exp Med* 1996; **183**:2593–603.

19 Loong CC, Hsieh HG, Lui WY, Chen A, Lin CY. Evidence for the early involvement of interleukin 17 in human and experimental renal allograft rejection. *J Pathol* 2002; **197**:322–32.

20 Van Kooten C, Boonstra JG, Paape ME *et al.* Interleukin-17 activates human renal epithelial cells in vitro and is expressed during renal allograft rejection. *J Am Soc Nephrol* 1998; **9**:1526–34.

21 Vanaudenaerde BM, Dupont LJ, Wuyts WA *et al.* The role of interleukin-17 during acute rejection after lung transplantation. *Eur Respir J* 2006; **27**:779–87.

22 Ivanov II, McKenzie BS, Zhou L, Tadokoro CE, Lepelley A, Lafaille JJ, Cua DJ, Littman DR. The orphan nuclear receptor RORgammat directs the differentiation program of proinflammatory IL-17+ T helper cells. *Cell* 2006; **126**:1121–33.

23 Langrish CL, Chen Y, Blumenschein WM *et al.* IL-23 drives a pathogenic T cell population that induces autoimmune inflammation. *J Exp Med* 2005; **201**:233–40.

24 Oppmann B, Lesley R, Blom B *et al.* Novel p19 protein engages IL-12p40 to form a cytokine, IL-23, with biological activities similar as well as distinct from IL-12. *Immunity* 2000; **13**: 715–25.

25 Dieckmann D, Plottner H, Berchtold S, Berger T, Schuler G. Ex vivo isolation and characterization of CD4(+) CD25(+) T cells with regulatory properties from human blood. *J Exp Med* 2001; **193**:1303–10.

26 Wing K, Lindgren S, Kollberg G, Lundgren A, Harris RA, Rudin A, Lundin S, Suri-Payer E. CD4 T cell activation by myelin oligodendrocyte glycoprotein is suppressed by adult but not cord blood CD25+ T cells. *Eur J Immunol* 2003; **33**:579–87.

27 Wan YY, Flavell RA. Identifying Foxp3-expressing suppressor T cells with a bicistronic reporter. *Pro Natl Acad Sci USA* 2005; **102**:5126–31.

28 Read S, Greenwald R, Izcue A, Robinson N, Mandelbrot D, Francisco L, Sharpe AH, Powrie F. Blockade of CTLA-4 on CD4+ CD25+ regulatory T cells abrogates their function in vivo. *J Immunol* 2006; **177**:4376–83.

29 Hack CJ. Integrated transcriptome and proteome data: the challenges ahead. *Brief Funct Genomic Proteomic* 2004; **3**:212–9.